Science of the Total Environment 795 (2021) 148728

Contents lists available at ScienceDirect

Science of the Total Environment

journal homepage: www.elsevier.com/locate/scitotenv

Compositional changes of $PM_{2.5}$ in NE Spain during 2009–2018: A trend analysis of the chemical composition and source apportionment

Marten in 't Veld [a,b,*], Andres Alastuey [a], Marco Pandolfi [a], Fulvio Amato [a], Noemi Pérez [a], Cristina Reche [a], Marta Via [a,c], María Cruz Minguillón [a], Miguel Escudero [d], Xavier Querol [a]

[a] Institute of Environmental Assessment and Water Research, IDAEA-CSIC, Barcelona 08034, Spain
[b] Department of Civil and Environmental Engineering, Universitat Politècnica de Catalunya, Barcelona 08034, Spain
[c] Department of Applied Physics, University of Barcelona, Barcelona 08028, Spain
[d] Centro Universitario de la Defensa, Academia General Militar, Zaragoza 50090, Spain

HIGHLIGHTS

- $PM_{2.5}$ levels decreased with $-2.8\%yr^{-1}$ at Barcelona and $-3.3\%yr^{-1}$ in Montseny
- Multisite PMF identified 9 common sources between the urban and rural stations
- Decrease driven by anthropogenic sources and secondary sulfate at both stations
- The relative contribution of secondary organic aerosols increased over 2009–2018
- Secondary organic aerosols is the biggest contributing source at both stations

GRAPHICAL ABSTRACT

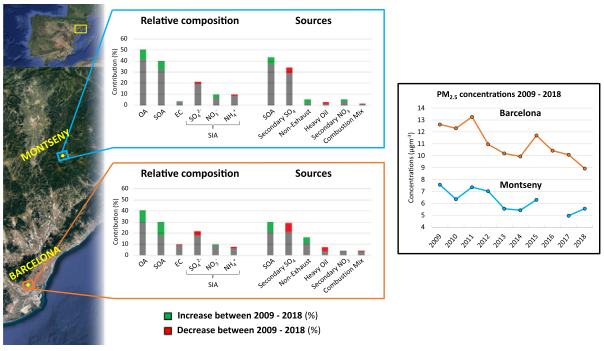

ARTICLE INFO

Article history:
Received 15 April 2021
Received in revised form 11 June 2021
Accepted 24 June 2021
Available online 28 June 2021

Editor: Pavlos Kassomenos

Keywords:
$PM_{2.5}$
Time-series analysis
Source apportionment
Multisite PMF
SOA

ABSTRACT

In this work, time-series analyses of the chemical composition and source contributions of $PM_{2.5}$ from an urban background station in Barcelona (BCN) and a rural background station in Montseny (MSY) in northeastern Spain from 2009 to 2018 were investigated and compared. A multisite positive matrix factorization analysis was used to compare the source contributions between the two stations, while the trends for both the chemical species and source contributions were studied using the Theil–Sen trend estimator. Between 2009 and 2018, both stations showed a statistically significant decrease in $PM_{2.5}$ concentrations, which was driven by the downward trends of levels of chemical species and anthropogenic source contributions, mainly from heavy oil combustion, mixed combustion, industry, and secondary sulfate. These source contributions showed a continuous decrease over the study period, signifying the continuing success of mitigation strategies, although the trends of heavy oil combustion and secondary sulfate have flattened since 2016. Secondary nitrate also followed a significant decreasing trend in BCN, while secondary organic aerosols (SOA) very slightly decreased in MSY. The observed decreasing trends, in combination with the absence of a trend for the organic aerosols (OA) at both stations, resulted in an increase in the relative proportion of OA in $PM_{2.5}$ by 12% in BCN and 9% in MSY, mostly from SOA, which increased by 7% in BCN and 4% in MSY. Thus, at the end of the study period, OA accounted for 40% and 50% of the annual mean $PM_{2.5}$ at BCN and MSY, respectively. This might have relevant implications for air quality policies aiming at abating $PM_{2.5}$ in the study region and for possible changes in toxicity of $PM_{2.5}$ due to marked changes in composition and source apportionment.

* Corresponding author at: Institute of Environmental Assessment and Water Research, IDAEA-CSIC, Barcelona 08034, Spain.
E-mail address: Marten.Veld@idaea.csic.es (M. Veld).

https://doi.org/10.1016/j.scitotenv.2021.148728

1. Introduction

Air pollution is a major environmental issue around the world (IHME, 2020, 2018; WHO, 2016). The World Health Organization (WHO) reported that, in 2016, more than 4.2 million premature deaths in the world (7.6% of all deaths) were in part attributable to air quality impairment by high levels of atmospheric particulate matter (PM) occurring every year (WHO, 2018). The European Environmental Agency (EEA, 2020) reported 379,000 premature deaths in EU-28 countries attributable to $PM_{2.5}$ (particulate matter of diameter < 2.5 μm) in 2018, 54,000 attributable to NO_2, and 19,400 attributable to O_3. However, various initiatives have forced a reduction in $PM_{2.5}$ concentrations since 1990, reducing the impact on mortality attributed to $PM_{2.5}$ by one third as of 2018 (EEA, 2020, 2018).

Moreover, apart from its effects on human health, PM also has climatic and ecological effects. The latter include direct deposition into the soil, which affects nutrient cycling; its acidic and alkaline content can cause leaf surface injury in plants (Grantz et al., 2003). These are major concerns as the impacts of PM on the environment and human health might increase with climate change (Dias et al., 2012; Ministerio para la Transición Ecológica, 2018). The health effects of these particles depend on their chemical compositions and physical properties (size, particle number, and surface area) (WHO, 2013). The chemical composition of PM is an important factor that determines its toxicity (Jia et al., 2017). The composition of $PM_{2.5}$ consists of a multitude of primary and secondary components, containing variable proportions of carbonaceous compounds, metals, and salts, depending on the major emission sources and the atmospheric conditions driving the variability of PM levels at a given site (Jia et al., 2017; H. Zhang et al., 2018a).

As PM is a pollutant harmful to health and the environment, efforts have been made to reduce ambient levels of PM during the last few decades. The European Aerosols Monitoring and Evaluation Program (EMEP) evaluated air quality trends for 1990–2012 in Europe, finding a decrease of approximately 30% for both PM_{10} and $PM_{2.5}$ between 2000 and 2012 and reductions of 60% to 90% and 30% to 40% for sulfate (SO_4^{2-})- and nitrate (NO_3^-)-bearing pollutants in PM_{10}, respectively (EMEP/CCC, 2016; ETC/ACM, 2016). In spite of this decrease in the levels of PM and gaseous pollutants, EEA (2020) reported that in 2018, 48% and 74% of the EU-28 urban population were exposed to PM_{10} and $PM_{2.5}$ concentrations that exceeded the WHO Air Quality Guidelines (AQG) (WHO, 2006) of 20 μgm^{-3} for annual average PM_{10} and 10 μgm^{-3} for annual average $PM_{2.5}$, respectively.

In Spain, a number of policy actions have been implemented to achieve a significant reduction in PM pollution, as described elsewhere (Pandolfi et al., 2016; Querol et al., 2014). The 2000–2012 decreasing trend in PM_{10} and $PM_{2.5}$ for Spain was observed and interpreted by Querol et al. (2014). They reported a gradual decrease until 2008, when a marked drop in concentrations was measured, after which (since 2010) the concentrations did not change significantly, likely indicating the attainment of a lower limit. Similar trends were seen for other major pollutants, such as SO_2, NO_2, and NO_x.

While the ambient concentrations have been reduced over time, the relative toxicity of PM (normalized per unit of concentration) may or may not have varied because this depends upon the PM chemical composition (Jia et al., 2017). Thus, because emissions of SO_2 and, in lower proportions, NO_x have decreased, the concentrations of SO_4^{2-} and NO_3^- might have decreased in $PM_{2.5}$ with time when compared with other PM components. This may have resulted in increased relative concentrations of more toxic compounds in $PM_{2.5}$. Although currently no clear hierarchy in toxicity of PM components has been found due to their complex compositions and interactions with other pollutants, studies have indicated that organic carbon (OC), elemental carbon (EC), and metals such as Ni and V appear to have a larger impact on the overall toxicity of $PM_{2.5}$, while there is less evidence to connect secondary inorganic aerosols (SIA) with health effects in laboratory studies (Hime et al., 2018; Kelly and Fussell, 2012; Park et al., 2018) and epidemiology studies (Bell et al., 2014; W. Zhang et al., 2018b). Nevertheless, WHO (2013) stated that SIA species also may have health effects associated with them.

W. Zhang et al. (2018b) demonstrated for New York State in the USA that even if the premature mortality attributable to $PM_{2.5}$ markedly decreased in parallel with the ambient $PM_{2.5}$ abatements, the normalized excess risk rate for premature mortality increased by a factor of 3 for $PM_{2.5}$ for the period 2014–2016 compared to 2005–2013. This was most likely caused by a change in relative composition in $PM_{2.5}$, mostly attributed to the increase in relative secondary organic carbon (SOC), which is a strong oxidant (Emami et al., 2018; Squizzato et al., 2018; W. Zhang et al., 2018b). Jiang et al. (2016) found that anthropogenic aged secondary organic aerosols (SOA) have a relatively high oxidative potential compared with other PM components. Similar results have been found by Tuet et al. (2017), Arashiro et al. (2018), Wang et al. (2018), Chowdhury et al. (2019), and Daellenbach et al. (2020), among others. SOA is closely linked to ozone (O_3), whose urban concentrations increased over the years (Querol et al., 2014, 2016). The higher O_3 levels increased the readily available hydroxyl and nitrate oxidizing radicals ($OH^•$ and $NO_3^•$) in the urban atmosphere of Madrid by 60% and 100%, respectively, in the last 7 years (Saiz-Lopez et al., 2017). In addition, the decrease in SO_2 and NO_x in the cities also decreased the consumption of these oxidizing radicals to generate SIA, so that more oxidizing radicals were available, which creates an environment more prone to generating SOA. In fact, Via et al. (2021) compared measurements with an Aerosol Chemical Speciation Monitor (ACSM) between May 2014–May 2015 and Sep 2017–Oct 2018 in Barcelona, showing an increase in the relative content of SOA in particulate matter of diameter < 1 μm (PM_1) and a higher degree of oxidation in the later period. Two other factors might have contributed to a higher relative proportion of OC, and especially SOA, in $PM_{2.5}$. First, an increase in the number of sport utility vehicles (SUV) in the global vehicle fleet might have resulted in enhanced SOA formation due to the higher emission rates of volatile organic compounds (VOC) and NO_x (Frey, 2018; Zhao et al., 2017). Furthermore, most cars are now equipped with gasoline direct injection engines, which produce larger SOA mass concentrations (Wang et al., 2020). Second, the increase in domestic biomass burning in Europe might have accounted for an increase in emissions of organic matter-enriched PM (EEA, 2018). These are all sources and processes for emission and generation of carbonaceous material, potentially producing more toxic $PM_{2.5}$ (Cassee et al., 2013; Jia et al., 2017; Kelly and Fussell, 2012).

This paper focuses on northeastern (NE) Spain, an area that has been identified as one of the regions recording the highest O_3 levels in Spain (Querol et al., 2016). We specifically focus on Barcelona (BCN) (NE Spain; 4.6 million inhabitants in the metropolitan area), which is a seaside city with numerous anthropogenic emission sources of air pollutants, such as road traffic, industrial plants, and shipping (Amato et al., 2016; Pandolfi et al., 2020), and on the Montseny (MSY) Massif northeast of Barcelona (Cusack et al., 2012; Pandolfi et al., 2016). A previous comparison of the trends in $PM_{2.5}$ levels and compositions in BCN and MSY was performed by Pandolfi et al. (2016), but they were not able to determine the trends for most primary PM components in BCN as these were affected by the relocation of the BCN station in 2008 to approximately 600 m north of the previous location, which mostly influenced the mineral components and consequently the trends in both PM_{10} and $PM_{2.5}$. To the authors' knowledge, this will be the most recent long-term comparison between the two stations since the relocation of the BCN station.

The main aim of this paper is to evaluate a time-series analysis of the chemical species and source contributions of $PM_{2.5}$ between 2009 and 2018 in NE Spain to determine if the relative composition of $PM_{2.5}$ has changed during this period. Data on $PM_{2.5}$ concentrations and chemical compositions were obtained from the above twin urban and regional background stations and were evaluated using the Theil–Sen trend estimator to determine the trends. A positive matrix factorization (PMF)

model was used to apportion $PM_{2.5}$ concentrations into main sources/factors at both stations. These results are expected to give insight into the causes of changes in the levels and chemistry of $PM_{2.5}$ over this time period, and therefore to yield relevant information for improving the efficiency of further pollution abatement actions.

2. Methodology

2.1. Measurement stations and sampling protocol

Barcelona is located in NE Spain, in a narrow corridor between the Mediterranean Sea to the east and the Collserola Mountains to the west. With 4.6 million inhabitants in the metropolitan area and 1.7 million in the city, it is the second biggest city in Spain and the fifth most populous urban area in the European Union (Demographia World Urban Areas, 2020). The emissions from the city are characterized by various industrial zones, power plants, a harbor, and road traffic, making it one of the areas with the highest density of atmospheric pollutant emissions in the Western Mediterranean Basin (WMB) (Amato et al., 2009b; Pandolfi et al., 2016; Querol et al., 2004a, 2004b, 2014). The BCN urban background station is located in the city of Barcelona (Fig. 1, red), within the Consejo Superior de Investigaciones Científicas institute (41°23′14.5"N, 2°06′55.6″E, 68 m a.s.l.). The location of the site is in proximity of Diagonal Avenue (Fig. 1, in black), which is one of the main traffic arteries of the city. The distance from Diagonal Avenue (220 m) is enough to be considered as an urban background site. However, when sea breezes are developed, traffic pollution from Diagonal Avenue might influence PM levels at the site. It is worth noting that the monitoring station was moved to a new location in 2012 (approximately 200 m to the west), but this did not affect concentrations significantly, as the immediate environments of both locations are similar. The MSY station (Fig. 1, green) is located at the Montseny Massif (41°46′45.63"N, 02°21′28.92″E, 720 m a.s.l.), and is representative of the regional background of the WMB. The station is 50 km northeast of BCN and 25 km from the Mediterranean coast. The station is part of the European Aerosols, Clouds, and Trace Gases Research Infrastructure Network (ACTRIS) and the Global Atmosphere Watch (GAW).

The period considered for the present study is from 04/01/2009 to 29/12/2018. $PM_{2.5}$ samples were collected over a period of 24 h at a sampling rate of 1 every 4 days simultaneously at the BCN and MSY stations. Sampling was carried out by using DIGITEL and MCV high volume samplers (30 m^3h^{-1} in both cases) and 15 cm diameter Pall ultrapure quartz microfiber filters.

To prevent selection bias and interference from the North African dust (NAF) episodes affecting NE Spain, 98 samples from days with dust outbreaks over BCN, determined according to EU guidelines (European Commission, 2011), have been removed from the dataset to improve the quality of the trend analysis and modeling. Additionally, the gaps in the dataset can produce a yearly or seasonal bias in the data. To prevent this, years and/or seasons were removed from their respective trend analyses if less than 75% of the samples (at a sampling rate of 1 sample every 4 days) were available in the given year or season. For both stations, 75% represents at least 70 samples on a yearly basis and at least 15 samples on a seasonal basis. These requirements resulted in the removal of autumn 2010 from the seasonal averages of BCN and the removal of the summers of 2016 and 2017 from the seasonal trend analysis of MSY. Furthermore, 2016 was also removed from the yearly trend analysis of MSY. In total, 852 samples were used for the BCN trend analysis and 633 for the MSY trend analysis during the period of 2009 to 2018. Table S2 shows the number of samples selected at each station per month.

2.2. Chemical composition data

The filters were cut into four quarters for subsequent analyses. An area of 1.5 cm^2 was punched from one quarter to measure the levels of OC and EC by thermal-optical carbon analyzer (SUNSET), using the EUSAAR 2 protocol (Cavalli and Putaud, 2010). The second quarter underwent acid digestion with HNO_3:HF:$HClO_4$ (2.5:5.0:2.5 mL) according to the protocol of Querol et al. (2001b). The resulting solutions were analyzed using an inductively coupled plasma atomic emission

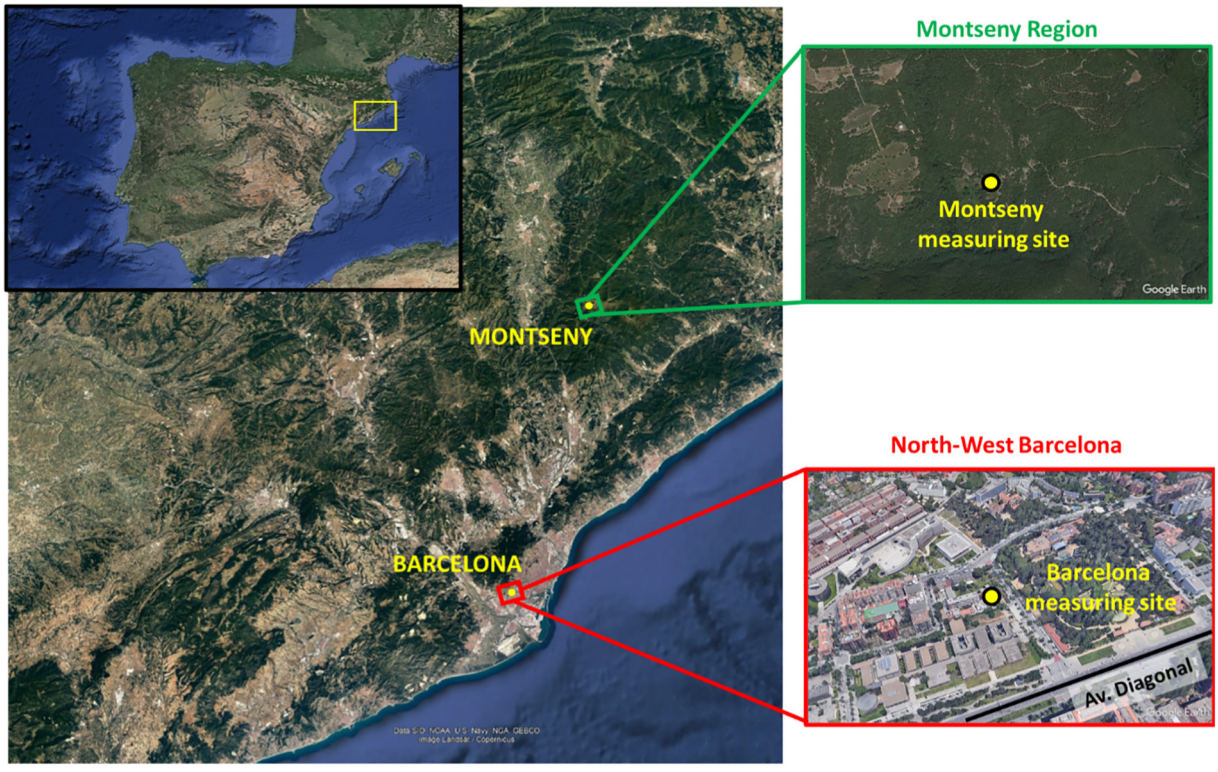

Fig. 1. The locations of the Barcelona (BCN) urban station (41°23′14.5"N 2°06′55.6″E, 68 m a.s.l.) and the Montseny rural (MSY) station (41°46′45.63"N, 02°21′28.92″E, 720 m a.s.l.), located in NE Spain, in the Catalunya region. Images were obtained from Google Earth.

spectrometer (ICP-AES, ICAP 6500 Radial View, Thermo Fisher Scientific) to determine the concentrations of major elements and a number of trace elements (Al, Ba, Ca, Fe, K, Mg, Mn, Na, P, S, Ti, V, and Zn); and with an inductively coupled plasma mass spectrometer (ICP-MS, iCAP-RQ, Thermo Fisher Scientific) for trace elements (Li, Be, B, Sc, Ti, V, Cr, Mn, Co, Ni, Cu, Zn, Ga, Ge, As, Se, Rb, Sr, Y, Zr, Nb, Mo, Cd, Sn, Sb, Cs, Ba, La, Ce, Pr, Nd, Sm, Eu, Gd, Tb, Dy, Ho, Er, Tm, Yb, Lu, Hf, Ta, W, Tl, Pb, Bi, Th, and U). The third quarter was leached in 30 mL of Milli-Q water for 6 h to determine the concentrations of NO_3^-, SO_4^{2-}, and Cl^- using ion chromatography (IC). A change in IC instrumentation occurred in 2015 from the Waters 1525 HPLC Pump (Water Corporation) to the Dionex Aquion (Thermo Fisher Scientific). The difference between the two pieces of equipment was significant due to the different sample pre-treatments, reagents, standards, columns, detectors, and software. To determine the impact of this change, a year-long comparison was made between the results of a co-located ACSM (Q-ACSM, Aerodyne Inc.) for PM_1 in 2014–2015 and 2017–2018 in BCN and PM_1 filter samples during the same periods. The method used for the ACSM was described by Via et al. (2021). In the comparison of the two methods, SO_4^{2-} showed good agreement with the ACSM results; the slope of the relationship between SO_4^{2-} concentrations from the filters and the ACSM was 1.13 (R^2 = 0.87) in 2014–2015 and 0.95 (R^2 = 0.91) in 2017–2018. NO_3^- also showed good agreement, giving a slope of 1.57 (R^2 = 0.91) in 2014–2015 and 1.62 (R^2 = 0.84) in 2017–2018. The higher concentrations of NO_3^- of the ACSM is due to the loss of nitrate during filter sampling and the ACSM including organic nitrate (Chow et al., 2005). In both cases, the good correlation in both periods implies that the instrumentation change had no major effects on the results for NO_3^- and SO_4^{2-}. The Cl^- concentrations, however, showed poor agreement, with a slope of 0.05 (R^2 = 0.18) in 2014–2015 and 18.67 (R^2 = 0.17) in 2017–2018. The dramatic change in slope implies that the instrumentation change had a major impact on the Cl^- concentration, but the poor correlation with the ACSM in both periods means we cannot determine which of the three measurements is correct. Hence, the Cl^- results for the whole period were not included in the analysis. Finally, NH_4^+ was determined in the leachates by using an ion-specific NH_4^+ electrode (ORION 9512HPBNWP ammonium selective electrode, Thermo Fisher Scientific) and potentiometer (ORION 4Star potentiometer, Thermo Fisher Scientific). The remaining quarter of each sample was archived. Finally, the $PM_{2.5}$ concentrations were calculated using the sum of the chemical species. The more common gravimetrical mass method includes unaccounted PM mass that the sum of the chemical species analyzed here does not include, such as non-C atoms in organic aerosols (OA) and/or measurement artifacts. However, the unaccounted mass also includes unwanted artifacts, as a part of the unaccounted mass originates from the influence of moisture and the formation and crystallization of water on particles. This artifact will increase the weight of the filter, which in turn will affect the gravimetrical determination of $PM_{2.5}$ (Tsyro, 2005). Tsyro (2005) determined that the particle-bound water could constitute 20% to 35% of annual $PM_{2.5}$ concentrations. Including the unaccounted mass in the research would obstruct the analysis of trends, especially trends in the relative composition as it could reach in a number of samples up to 50% of the chemical composition (especially in the period 2016–2018), which origin is unknown but related to the humidity control in weighting samples. A comparison between the $PM_{2.5}$ concentrations (without unaccounted mass) for the BCN site with the one from the same site including the unaccounted and with those from two official urban background AQ monitoring sites is presented in Fig. S1.

2.3. Indirect calculations

Various PM components used for the determination of the $PM_{2.5}$ chemical composition were determined indirectly from other direct measurements.

The OA and EC concentrations were calculated according to the calculations from Turpin (Eqs. (1)–(4)), who determined that OC should be multiplied by 1.7 in urban areas and by 2.1 in rural areas to estimate OA (Turpin et al., 1997; Turpin and Lim, 2001). These values are close to the experimentally determined values of 1.6 in BCN (Mohr et al., 2012) and 2.0 in MSY (Minguillón et al., 2011), which were determined between February and March 2009.

$$(OA + EC) = n * OC + 1.1 * EC \quad (1)$$

$$OA_{urban} = 1.7 * OC \quad (2)$$

$$OA_{rural} = 2.1 * OC \quad (3)$$

$$EC_{total} = 1.1 * EC \quad (4)$$

The SOA was calculated using the EC tracer method, which has been used in previous studies to estimate SOA concentrations (Castro et al., 1999; Dinoi et al., 2017; Wu and Yu, 2016; Yu et al., 2004). This method calculates the SOA according to the following equation:

$$SOA = OA - \left(\frac{OC}{EC}\right)_{min} * EC \quad (5)$$

The $(OC/EC)_{min}$ was determined by taking the 2nd percentile of OC/EC ratios at BCN and MSY, which corresponded to 1.16 for BCN and 2.92 for MSY.

Some of the measured compounds can originate from both sea salt and from the crust of the Earth. Therefore, various indirect calculations were performed on the Na, Ca, Mg, K, and SO_4^{2-} measurements to estimate the amount originating from sea salt (ss) and the crustal layer (dust). The Na_{dust} concentration was estimated by multiplying the concentrations of Al, which has no sea salt origin, by the ratio of Na/Al in the crust (Haynes et al., 2017). Once Na_{dust} is calculated, it is possible to calculate the Na_{ss}:

$$Na_{dust} = Al * 0.287 \quad (6)$$

$$Na_{ss} = Na_{total} - Na_{dust} \quad (7)$$

K_{dust} values were calculated using the same method.

$$K_{dust} = Al * 0.254 \quad (8)$$

The calculated concentrations of Na_{ss} were then used to calculate the concentrations of SO_{4ss}^{2-}, Ca_{ss}, Mg_{ss}, and K_{ss}, based on the known ratios between Na and each chemical in seawater (DOE, 1992).

$$SO_4^{2-}{}_{ss} = Na_{ss} * 0.273 \quad (9)$$

$$Ca_{ss} = Na_{ss} * 0.037 \quad (10)$$

$$K_{ss} = Na_{ss} * 0.037 \quad (11)$$

$$Mg_{ss} = Na_{ss} * 0.120 \quad (12)$$

With these values obtained, the concentration of the crustal concentrations could be calculated for each of the remaining compounds.

$$Ca_{dust} = Ca_{total} - Ca_{ss} \quad (13)$$

$$Mg_{dust} = Mg_{total} - Mg_{ss} \quad (14)$$

The non-sea salt (nss) SO_4^{2-} could be determined in a similar manner.

$$SO_4^{2-}{}_{nss} = SO_4^{2-}{}_{total} - SO_4^{2-}{}_{ss} \quad (15)$$

K could also be used as a biomass burning tracer (K_{bb}) and was calculated as the difference between measured K and the sum of K_{ss} and K_{dust} (Pachon et al., 2013; Reche et al., 2012; Yu et al., 2018).

$$K_{bb} = K_{total} - K_{ss} - K_{dust} \quad (16)$$

The concentrations of the carbonates in the crustal matter were calculated using stoichiometric ratios.

$$Al_2O_3 = 1.8868 * Al_{dust} \quad (17)$$

$$Fe_2O_3 = 1.4297 * Fe_{dust} \quad (18)$$

$$TiO_2 = 1.6685 * Ti_{dust} \quad (19)$$

$$CaO = 1.3992 * Ca_{dust} \quad (20)$$

$$MgO = 1.6583 * Mg_{dust} \quad (21)$$

$$K_2O = 1.2046 * K_{dust} \quad (22)$$

$$P_2O_5 = 2.2914 * P_{dust} \quad (23)$$

Finally, SiO_2 concentrations were indirectly estimated from Al_2O_3 concentrations (Querol et al., 2019).

$$SiO_2 = 2.5 * Al_2O_3 \quad (24)$$

2.4. Theil–Sen trend estimation

To statistically assess the pollution trends over the years, the Theil–Sen estimator was used (Sen, 1968; Theil, 1950). This method estimates the slope between N pairs of x, y values in the dataset and computes the slope between all pairs of points. The Theil–Sen estimate of the slope is the median of all the slopes (Carslaw, 2019). In this paper, the trends are based on a yearly average to determine the trend between 2009 and 2018 but also on a seasonal average to determine trends that occur during certain seasons and/or to avoid seasonal influences on certain species. The values of the Theil–Sen trend estimation were obtained using the OpenAir software package in R (Carslaw, 2019; Carslaw and Ropkins, 2012).

The trends in the chemical composition were separated into different groups of chemicals:

1) OA and one of its constituents, SOA.
2) EC.
3) SIA, which consists of NO_3^-, NH_4^+, and SO_{4nss}^{2-}.
4) Mineral aerosols, calculated as the sum of CO_3^{2-}, Al_2O_3, SiO_2, Fe_2O_3, MgO_{dust}, Na_2O_{dust}, K_2O_{dust}, TiO_2, P_2O_5, MnO, and Ca_{dust}.
5) Sea spray aerosols, which include Na_{ss}, Ca_{ss}, K_{ss}, Mg_{ss}, and SO_{4ss}^{2-}.
6) The sum of the trace elements (excluding P, Ti, and Mn, as these are included in the indirect calculations of the mineral aerosols). Only the few constituents of the trace elements that have significant trends and are known to be tracers of specific sources of PM will be discussed in the trend analysis.
7) Biomass burning, traced by K_{bb}.

For the seasonal trend analysis, the seasons are divided into spring (March, April, May), summer (June, July, August), autumn (September, October, November), and winter (December, January, February). In this study, December was considered to belong to the winter of the next year (i.e., December 2014 was considered winter 2015).

2.5. Positive matrix factorization

A PMF model (Paatero and Tapper, 1994) was applied using the PMFv5.0 software (EPA, Norris et al., 2014). PMF is a multivariate factor analysis tool that decomposes a matrix, in this case $PM_{2.5}$ chemical compositions on different days, into two matrices: factor contributions and factor profiles. With these results, the PMF model could be used to identify the sources and the quantities of their contributions to the collected $PM_{2.5}$. The uncertainties and detection limits of the different species were calculated as described by Amato et al. (2009a) and Escrig Vidal et al. (2009). The analytical uncertainties, the standard deviations of the different species in the blank filters, and the % above detection limit were considered in the uncertainty calculations.

To select species to be included in the model, a signal to noise (S/N) ratio of >1.5 was defined as a criterion indicating a strong species, while an S/N ratio between 1.5 and 0.5 indicated a weak species. Weak species' uncertainties were increased by a factor of 3. In total, three separate PMF analyses were performed: one for each station separately and a multisite analysis with both stations in which both datasets were combined into a single dataset. The main advantage of the multisite PMF is that this analysis includes a larger dataset compared to the separate single-site PMF models and that the profiles to compare sites are the same. This will produce more robust results, allowing us to include source contributions with low concentrations that could not be identified in a single-site PMF, and the identified sources will represent the sources that affect both sampling sites and will focus more on general phenomena instead of local variations. Constraints in this analysis exist due to the distance between the two stations, possible differences in sources, and different source profiles for the same sources (Escrig Vidal et al., 2009). Pandolfi et al. (2020) has previously demonstrated the feasibility of using the multisite PMF for this study area. The species included for each PMF are listed in Table S3, but a few exceptions to the stated criteria were included in the analysis. In the BCN PMF, Cl^- has been excluded, as noted earlier in this section, even though it had a S/N ratio of 0.5. Furthermore, Al had a low S/N ratio but is a known tracer for mineral aerosols and was therefore included as a weak species. Finally, both Sn and Se were removed from the data set. In the case of Se, this was due to the lower analytical noise after installation of a collision cell in the ICP-MS in early 2018, and in the case of Sn, its inclusion resulted in a "ghost" Sn factor in PMF, without any physical meaning.

In the MSY PMF, Cl^- and Se were removed for the same reasons as in BCN. In addition, a few tracers such as Al, K, and Ni were added as weak species even though they had S/N ratios below 0.5, because these species are known tracers in BCN and MSY (Amato et al., 2009a, 2009b; Brines et al., 2019; Pandolfi et al., 2016; Pérez et al., 2016).

For the combined multisite PMF analysis, from the elements having S/N < 0.5, only Al was included, and Se and Sn were again excluded for the same aforementioned reasons. The inclusion of the known traces (Al, K, Ni) aided with identifying the sources, but their inclusion had no significant impact on any of the PMF solution, as removing them resulted in the same solution being presented.

Every model underwent 50 runs with 117 as the seed number. The optimal number of sources was selected by inspecting Q values, residuals, G space plots, and the physical meaning of the factors using previous expertise on PMF results in BCN and MSY. To confirm the optimal factor profiles of the PMF model, the data was also bootstrapped. Each dataset was bootstrapped 100 times with a minimum correlation R-value of 0.6. Finally, the model error was estimated using the base model displacement method. The results from the PMF analysis were also used in a Theil–Sen trend estimation to determine the trends of the source contributions.

2.6. SOA source verification

In the PMF analysis, most sources had been previously detected in BCN and MSY (Amato et al., 2016, 2009b; Cusack et al., 2012; Pandolfi et al., 2016; Pérez et al., 2016; Pey et al., 2013; Querol et al., 2004a, 2007, 2008, 2009a, 2009b, 2014) and were therefore identified based on prior knowledge. However, the SOA source has not been previously identified as a separate source when using PM filter samples without the use of additional organic compounds (Brines et al., 2019). Although the source was detected in the current study, it might be a well-known positive OC artifact from the trapping of VOCs by the quartz fibers,

forming artifact SOA (Kirchstetter et al., 2001; Watson et al., 2009). To evaluate this, a correlation study was performed between the SOA source contribution in $PM_{2.5}$ from the present PMF analysis and the SOA contribution in PM_1 determined from ACSM data for overlapping periods. The comparison period was from 21/09/2017 to 31/10/2018 for the BCN station (Via et al., 2021) and from 14/06/2012 to 09/07/2013 for the MSY station (Minguillón et al., 2015).

3. Results

3.1. 2009–2018 trend analysis

Table 1 summarize the results of the Theil–Sen trend estimation of the major and trace components of $PM_{2.5}$ for BCN and MSY. The complete Theil–Sen trend estimations are presented in Appendix A.

- The annual mean $PM_{2.5}$ concentrations in BCN and MSY showed statistically significant decreases of $-2.8\%\ yr^{-1}$ and $-3.3\%\ yr^{-1}$ between 2009 and 2018, respectively. The seasonal averages showed that there was only a statistically significant decrease during spring and summer in BCN, and during spring and autumn in MSY.
- The SIA showed a statistically significant decrease of $-4.9\%\ yr^{-1}$ in BCN and $-3.5\%\ yr^{-1}$ in MSY. This trend was significant during all seasons except winter in BCN, and during spring and summer in MSY. These decreasing trends were mostly driven by SO_{4nss}^{2-}, which decreased by $-5.1\%\ yr^{-1}$ and $-4.0\%\ yr^{-1}$ for BCN and MSY, respectively, on an annual basis. The decreasing trend is a result of various SO_2 (and then associated secondary sulfate) abatement strategies in power generation, shipping and industry, which have worked efficiently on both a local and regional level (European Parliament; Council of the European Union, 2001; Pandolfi et al., 2016; Pérez et al., 2016; Querol et al., 2009a, 2014; Viana et al., 2014). SO_{4nss}^{2-} also showed a seasonal pattern with higher concentration in the warmer months, and lower concentrations during the colder months at both stations. This seasonal variability is caused by the low oxidation ratios of SO_2 (the precursor to SO_{4nss}^{2-}) during winter of $<1\%\ h^{-1}$ compared to $6\%\ h^{-1}$ in the summer in the Mediterranean area (Querol et al., 1999a, 1999b). By contrast, NO_3^- showed the most moderate decrease with $-3.2\%\ yr^{-1}$ in BCN, only significant during spring, and no statistically significant trends in MSY. The difference in trends is attributed to the fact that NO_x, the precursor to NO_3^-, has a mostly anthropogenic origin, originating mainly from traffic in BCN but also from power generation, industry, and the domestic sector (Pandolfi et al., 2020, 2016). Various initiatives to reduce NO_x emissions in BCN had a significant impact in abating NO_x, decreasing NO concentrations by −28.8% and NO_2 by −20.6% between 2005 and 2017 (Massagué et al., 2019; Pandolfi et al., 2016). But due to its distance from the city, MSY was not significantly affected by these changes. Finally, NH_4^+ followed an intermediate trend that was closer to the one described for SO_{4nss}^{2-}, with annual decreasing trends of $-5.9\%\ yr^{-1}$ and $-2.2\%\ yr^{-1}$ for BCN and MSY, respectively. Both stations showed the most marked decreases in spring, but a statistically significant decrease was also observed during the summer in BCN.
- For the carbonaceous aerosol components, no statistically significant trends were identified for the annual trends of OA, SOA, or EC in

Table 1
Concentrations (in $\mu g\ m^{-3}$) of $PM_{2.5}$ and its chemical constituents in 2009 and 2018 and their respective Theil-Senn trend estimate ($\%yr^{-1}$) between 2009-2018 based on the annual averaged and seasonal averaged data in BCN (top) and MSY (bottom) between 2009 and 2018. The statistical significance is represented by *** for $p < 0.001$, ** for $p < 0.01$, * for $p < 0.05$, + for $p < 0.1$, and ns for not significant. The trends are presented on the annual data, but also the season specific data.

Barcelona	Concentrations ($\mu g\ m^{-3}$)		Annual trends ($\mu g\ m^{-3}\ yr^{-1}$) (α)		Seasonal trends ($\mu g\ m^{-3}\ yr^{-1}$) (α)							
Species	2009	2018	Annual		Autumn (SON)		Winter (DJF)		Spring (MAM)		Summer (JJA)	
$PM_{2.5}$	12.62	8.92	−0.33940	**	*ns*		*ns*		−0.64026	*	−0.35454	**
OA	3.57	3.55	*ns*		*ns*		*ns*		*ns*		*ns*	
SOA	2.21	2.63	*ns*		*ns*		*ns*		*ns*		*ns*	
EC	1.17	0.79	*ns*		*ns*		*ns*		*ns*		−0.02514	**
Crustal	1.86	1.08	*ns*		*ns*		*ns*		*ns*		*ns*	
Fe_2O_3	0.21	0.20	*ns*		*ns*		*ns*		*ns*		+0.00809	**
MnO	7.46×10^{-3}	4.43×10^{-3}	*ns*		*ns*		*ns*		*ns*		−0.00022	**
Na_{ss}	0.15	0.10	*ns*		−0.00779	+	*ns*		*ns*		*ns*	
SIA	5.08	3.2	−0.23337	*	−0.12274	+	*ns*		−0.44991	***	−0.18916	*
SO_{4nss}^{2-}	2.63	1.63	−0.12244	***	−0.10105	*	*ns*		−0.15926	**	*ns*	
NO_3^-	1.36	0.94	−0.04564	*	*ns*		*ns*		−0.14758	*	*ns*	
NH_4^+	1.09	0.63	−0.06337	***	*ns*		*ns*		−0.1914	***	−0.15522	*
Tracers	0.09	0.04	−0.00500	***	−0.00620	*	*ns*		−0.00620	*	−0.00460	*
V	6.61×10^{-3}	3.22×10^{-3}	−0.00033	**	−0.00044	**	*ns*		−0.00033	**	−0.00047	**
Ni	3.10×10^{-3}	1.20×10^{-3}	*ns*		−0.00015	*	*ns*		*ns*		*ns*	
K_{bb}	0.14	0.08	−0.01333	+	−0.01414	*	*ns*		*ns*		*ns*	
Montseny												
$PM_{2.5}$	7.54	5.55	−0.23501	**	−0.15255	*	−0.13999	*	−0.38486	**	*ns*	
OA	3.06	2.83	*ns*		*ns*		*ns*		*ns*		*ns*	
SOA	2.43	2.38	*ns*		*ns*		*ns*		*ns*		*ns*	
EC	0.21	0.15	−0.00469	*	*ns*		*ns*		*ns*		−0.00761	+
Crustal	0.58	0.38	*ns*		*ns*		*ns*		−0.03135	+	*ns*	
Al_2O_3	0.10	0.05	−0.00469	+	*ns*		*ns*		−0.00903	***	*ns*	
Fe_2O_3	0.05	0.04	*ns*		*ns*		*ns*		−0.00117	*	*ns*	
MnO	4.75×10^{-2}	1.34×10^{-3}	*ns*		*ns*		*ns*		*ns*		−0.00007	+
Na_2O_{dust}	0.02	0.01	−0.00143	+	*ns*		*ns*		−0.00185	***	*ns*	
K_2O_{dust}	0.02	0.01	−0.00113	+	*ns*		*ns*		−0.00146	***	*ns*	
TiO_2	6.88×10^{-3}	1.58×10^{-3}	−0.00037	***	−0.00033	+	*ns*		−0.00023	*	*ns*	
Na_{ss}	0.10	0.04	*ns*		−0.00363	**	−0.00506	*	*ns*		*ns*	
SIA	3.02	2.11	−0.10138	*	*ns*		*ns*		−0.13724	*	−0.19307	*
SO_{4nss}^{2-}	1.70	1.11	−0.06536	**	*ns*		*ns*		−0.09410	*	−0.14629	*
NH_4^+	0.80	0.50	−0.01267	+	*ns*		*ns*		−0.04026	*	*ns*	
Tracers	0.03	0.01	−0.00161	*	*ns*		−0.00162	*	−0.00191	*	*ns*	
V	1.62×10^{-3}	0.98×10^{-3}	−0.00008	**	*ns*		*ns*		*ns*		*ns*	
Ni	0.82×10^{-3}	0.20×10^{-3}	*ns*		*ns*		*ns*		$+1.76 \times 10^{-7}$	+	*ns*	

BCN. For MSY, only EC showed a statistically significant decrease. The seasonal concentrations of EC only followed a statistically significant decrease during summer at both stations.

- The mineral aerosols showed no statistically significant annual trends in both BCN and MSY, with only MSY showing a statistically significant decrease during spring. The lack of a trend in BCN is attributed to both the impact and recovery of the financial economic crises during the study period, as a part of the material arises from construction and demolition emissions (Amato et al., 2009a, 2016; Pandolfi et al., 2016; Querol et al., 2001a). Most of the major constituents did not show trends on a yearly basis, but some constituents showed statistically significant trends in the seasonal analysis (Table 1), mostly during spring in MSY and summer at both stations.
- K_2O_{bb} showed a statistically significant decreasing interannual trend of −6.7% in BCN, with a statistically significant decrease during autumn. The origin of this continuous decrease observed for Barcelona is unknown. The city has natural gas as major source for heating, being used for residential heating in about 96% of the homes (Amato et al., 2016). The progressive use of low emissions biomass stoves in the region and suburban areas might have caused this trend; however, no trends were observed in MSY. Biomass burning contributions to total OC was estimated using a combination of AMS-^{14}C tools in 14–15% in winter and 10–11% in summer for both sites (Minguillón et al., 2011).
- The sea spray aerosol trends cannot be discussed in this paper because of unreliable Cl^- data, as mentioned in the Methodology section (Section 2.2). Here, we only evaluated trends in Na_{ss}. As was expected, interannual trends for Na_{ss} were not evident for either BCN or MSY. Na_{ss} only showed a smooth statistically decrease of −5.7% yr^{-1} during autumn for both BCN and MSY, but also showed a statistically significant trend of −8.5% yr^{-1} during winter in MSY.
- The sum of all trace elements showed statistically significant decreases over the study period −5.2% yr^{-1} and −9.3% yr^{-1} for BCN and MSY, respectively. These decreases were seen in BCN during all seasons but winter and in MSY during spring and winter. One of the constituents, V, which together with Ni is a tracer for heavy oil combustion, showed a statistically significant decrease of −6.2% yr^{-1} in BCN and −5.4% yr^{-1} in MSY, which was seen over all seasons except winter in BCN and in summer and winter in MSY. Ni showed no statistically significant decrease. The seasonal trends showed a significant decrease of Ni only in autumn in MSY. The lack of a significant Ni decrease might indicate an additional source of Ni (such as metallurgy, see below).

Given the different trends followed by different $PM_{2.5}$ components, it is also necessary to evaluate the trends of the relative contributions of these to the bulk $PM_{2.5}$ concentrations. To this end, Table 2 presents the relative concentrations of each $PM_{2.5}$ major component and the existing significant trends on both an annual and seasonal basis.

3.2. $PM_{2.5}$ source contributions and their respective trends

The chemical profiles of all PMF analyses are presented in Fig. 2. These nine sources were all identified previously in either of the single-site PMFs of BCN and MSY. Eight major sources were identified for BCN (Fig. 2a; Fig. S2, left), with the secondary sulfate and SOA sources mixed together, while seven sources were identified for MSY (Fig. 2b; Fig. S2, right), as it was not possible to differentiate between non-exhaust vehicle emissions and combustion emissions because these are mixed when transported toward the regional background. This was also the case for the sea salt and the heavy oil combustion sources (mostly from shipping), which were mixed in the same source in MSY. In the multisite PMF, all these sources were identified separately. The bootstrap of all PMFs could correctly map the bootstrap factors to the base factors for over 96 out of 100 runs, with no errors found in the base model displacement method. The annual and seasonal Theil-Senn trends and the relative contribution of the nine sources are presented in Table 3. Furthermore, a direct comparison of the concentrations between 2009 and 2018 are presented in Fig. 3, while the seasonal variance of each source being presented in Fig. 4. The nine source contributions were identified, quantified, and listed below, in order of the largest to the smallest source.

1. SOA were traced by OC. This source contribution was attributed to secondary aerosols formed in the atmosphere from VOCs of both anthropogenic and biogenic origins. The secondary origin of this OC-rich source contribution was further supported by comparison with ACSM OOA data (end of Section 3.2). This source was only detected in the MSY PMF, whereas in BCN it was mixed with the secondary sulfate and traffic exhaust sources. The difference in the source profile between the multisite and the MSY PMFs was that in MSY there was a significant contribution of Ca, Na, and Mg attributed to this

Table 2
Relative composition of $PM_{2.5}$ chemical species (in %) in 2009 and 2018 and their respective Theil-Senn trend estimate (in %yr^{-1}) between 2009-2018 based on the annual averaged and seasonal averaged data in BCN (top) and in MSY (bottom) between 2009 and 2018. The bottom of the table states the statistically significant trends of each source, with the significance represented by *** for $p < 0.001$, ** for $p < 0.01$, * for $p < 0.05$, + for $p < 0.1$, and ns for not significant.

Barcelona	Relative composition		Annual trends (%yr^{-1}) (α)		Seasonal trends (%yr^{-1}) (α)							
Species	2009	2018	Annual		Autumn (SON)		Winter (DJF)		Spring (MAM)		Summer (JJA)	
OA	30%	41%	*ns*		+1.04	+	*ns*		+1.01	+	*ns*	
SOA	18%	30%	+0.65	*	+0.96	+	*ns*		*ns*		*ns*	
EC	10%	9%	*ns*		*ns*		*ns*		+0.23	*	*ns*	
Crustal	13%	12%	*ns*		*ns*		*ns*		+0.75	*	*ns*	
SIA	39%	34%	−1.03	*	*ns*		*ns*		−1.60	*	−0.87	**
SO_{4nss}^{2-}	22%	18%	−0.58	*	*ns*		−0.37	*	−0.65	*	−0.67	**
NO_3^-	9%	10%	*ns*		*ns*		*ns*		*ns*		*ns*	
NH_4^+	8%	7%	−0.29	**	*ns*		*ns*		−0.64	**	−0.25	*
Tracers	1%	1%	−0.04	+	−0.04	*	*ns*		−0.03	*	*ns*	
Montseny												
OA	41%	50%	*ns*		*ns*		*ns*		*ns*		+1.82	*
SOA	32%	40%	*ns*		*ns*		*ns*		*ns*		+1.94	*
EC	3%	3%	*ns*		*ns*		*ns*		*ns*		*ns*	
Crustal	8%	7%	*ns*		*ns*		*ns*		*ns*		*ns*	
SIA	37%	38%	*ns*		*ns*		*ns*		*ns*		−1.12	*
SO_{4nss}^{2-}	21%	19%	*ns*		*ns*		*ns*		*ns*		−1.05	*
NO_3^-	6%	10%	+0.41	*	*ns*		*ns*		*ns*		*ns*	
NH_4^+	10%	9%	*ns*		*ns*		*ns*		*ns*		*ns*	
Tracers	1%	0%	*ns*		*ns*		*ns*		*ns*		*ns*	

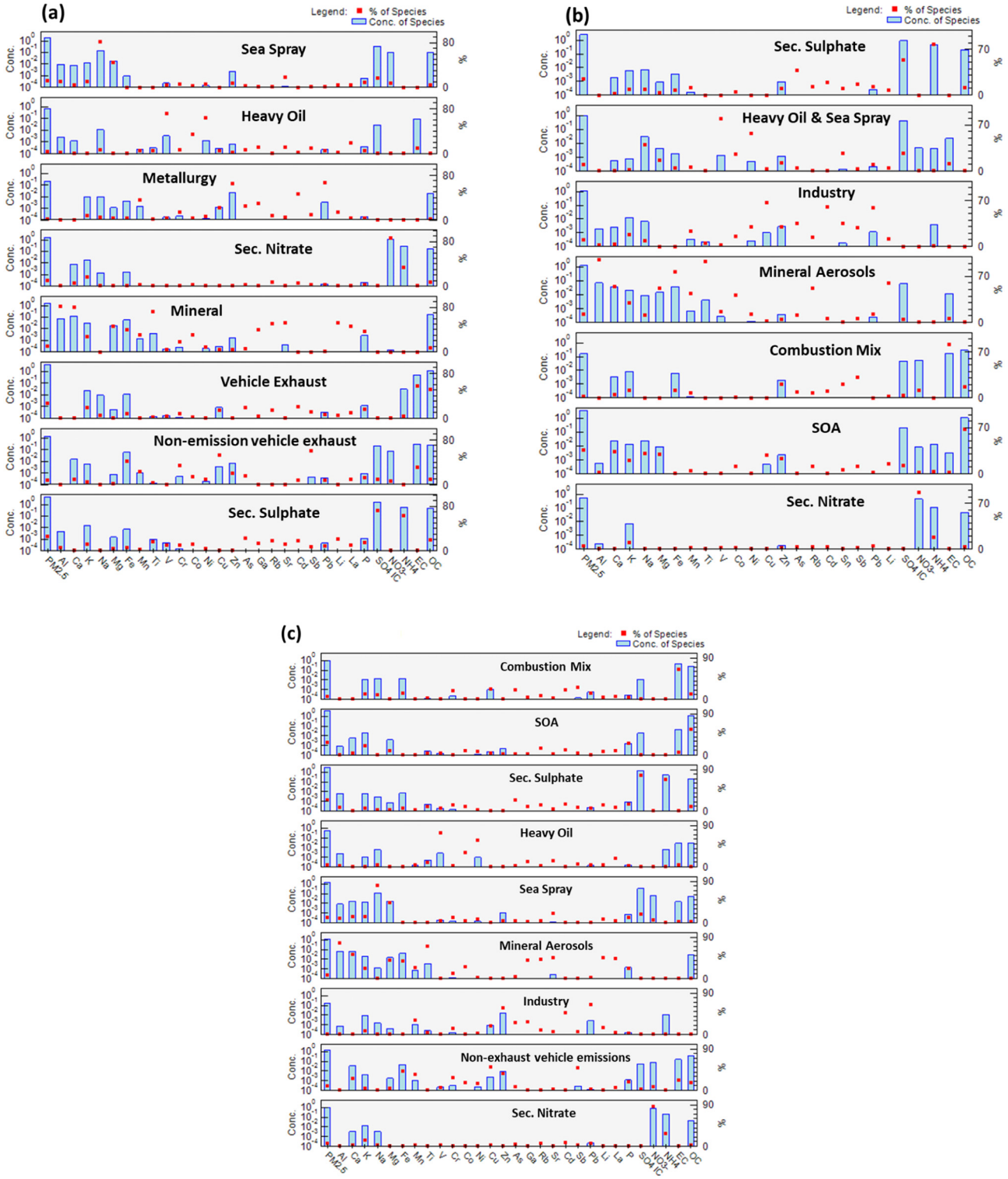

Fig. 2. Chemical profiles of the PMF analysis in (a) BCN, (b) MSY, and (c) the multisite analysis. Chemicals are shown on the x-axis; the concentrations at the source are shown on the y-axis, presented in blue bars in μgm^{-3}; relative contributions in % are shown as red squares on the secondary y-axis.

source that was not seen in the multisite PMF. The impact of this difference was only minor as similar average concentrations were found for this source contribution during 2009–2018 (with average concentrations being 3.2 μgm^{-3} and 3.7 μgm^{-3} for the MSY and multisite PMF, respectively). However, both solutions included a contribution of K to this source (20% in MSY and 14% in the multisite PMF). While the other minerals were removed from the multisite solution, the fact that K remained might indicate that a minor contribution of biomass burning is included in this solution (Viana et al., 2013). Biomass burning is discussed further in detail in Section 4.8. The solution from the multisite analysis did allow us to measure and evaluate the trends in secondary (anthropogenic + biogenic) OA in BCN. The seasonal variability of the two stations showed an opposing trend, with higher levels during the winter months in BCN,

Table 3
Theil-Senn trend estimate (%yr^{-1}) and relative contribution, and its respective trend, of the 9 PMF sources determined by the multisite PMF, between 2009-2018 based on the annual averaged and seasonal averaged data in BCN (top) and MSY (bottom) between 2009 and 2018. The resulting slope of the trend is presented in μgm^{-3}yr^{-1}, with its statistical significance represented by *** for p < 0.001, ** for p < 0.01, * for p < 0.05, + for p < 0.1, and ns for not significant.

Barcelona	Annual trends (μg m^{-3} yr^{-1}) (α)		Seasonal trends (μg m^{-3} yr^{-1}) (α)								Relative contribution			
Species	Annual		Autumn (SON)		Winter (DJF)		Spring (MAM)		Summer (JJA)		2009	2018	Trend (%yr^{-1}) (α)	
SOA	*ns*		*ns*		*ns*		*ns*		*ns*		21%	30%	*ns*	
Sec. SO_4	−0.3172	**	*ns*		*ns*		−0.4179	**	−0.2865	*	29%	21%	−1.3068	*
Sea Spray	*ns*		*ns*		*ns*		*ns*		*ns*		11%	10%	*ns*	
Non-exhaust	*ns*		*ns*		*ns*		*ns*		*ns*		11%	17%	+0.5744	+
Sec. NO_3	−0.0428	+	*ns*		−0.0212	*	*ns*		−0.0241	*	4.5%	4.6%	*ns*	
Crustal	*ns*		*ns*		*ns*		*ns*		*ns*		8.8%	10%	+0.6201	*
Heavy Oil	−0.0531	+	−0.0772	***	*ns*		−0.0513	**	−0.0895	*	7.3%	3.6%	−0.2066	+
Combustion	−0.0197	+	*ns*		*ns*		−0.1033	+	*ns*		4.5%	3.4%	*ns*	
Industry	−0.0277	***	−0.0251	*	−0.0245	*	−0.0365	***	−0.0250	**	2.2%	0.7%	−0.1689	**

Montseny	Annual trends (μg m^{-3} yr^{-1}) (α)		Seasonal trends (μg m^{-3} yr^{-1}) (α)								Relative contribution			
Species	Annual		Autumn (SON)		Winter (DJF)		Spring (MAM)		Summer (JJA)		2009	2018	Trend (%yr^{-1}) (α)	
SOA	−0.0521	*	*ns*		*ns*		*ns*		−0.0521	*	37%	44%	*ns*	
Sec. SO_4	−0.1458	*	*ns*		*ns*		−0.1745	*	−0.1458	*	34%	29%	*ns*	
Sea Spray	−0.0676	*	*ns*		*ns*		*ns*		−0.0676	*	9.8%	6.9%	*ns*	
Non-exhaust	*ns*		+0.0196	+	*ns*		*ns*		*ns*		1.9%	5.6%	*ns*	
Sec. NO_3	*ns*		*ns*		*ns*		*ns*		*ns*		3.4%	5.5%	*ns*	
Crustal	*ns*		*ns*		*ns*		*ns*		*ns*		8.5%	5.6%	*ns*	
Heavy Oil	−0.0160	*	-0.0098	+	−0.0114	*	*ns*		−0.0231	*	2.6%	1.2%	−0.1008	*
Combustion	−0.0034	+	*ns*		*ns*		*ns*		−0.0059	*	1.4%	1.2%	*ns*	
Industry	−0.0065	***	−0.0063	+	*ns*		−0.0094	*	−0.0029	*	1.3%	0.8%	−0.0392	+

compared to the higher levels during the summer months in MSY. This stark difference originates from the different sources of OC at each station. In BCN the sources of OC mostly originate from fossil fuel combustion, which has higher levels in winter compared to summer due to stronger accumulation of pollutants during the cold season with lower atmospheric dispersion, and higher fossil combustion for residential heating. Simultaneously, non-fossil OC at Barcelona also showed a seasonal variability due to higher contribution of biomass burning and reduced mixing in the winter (Minguillón et al., 2011; Querol et al., 2013). Meanwhile at MSY, the higher concentrations in the summer are a result of higher biogenic emissions of VOCs (Minguillón et al., 2011; Querol et al., 2009a, 2013; Seco et al., 2011), lower renewal of the atmospheric air masses at the regional scale in summer (L. Pérez et al., 2008b; Rodríguez et al., 2002), and higher secondary aerosol formation ratios due to enhanced summer photochemistry. Minguillón et al. (2011) confirmed this as well, concluding that ≈47% of the fossil-OC in BCN is primary while in MSY ≈ 85% is secondary. The source contribution at both stations stayed quite stable over the study period; higher contributions were found in BCN compared to MSY, with average concentrations of 4.3 μgm^{-3} (27%) and 3.7 μgm^{-3} (41%), respectively. A statistically significant decrease was found in MSY of −0.05 μgm^{-3} yr^{-1} (*; −1.4% yr^{-1}) on an interannual basis, but none was found during any particular season. It is very probable, as shown by Table 3, that there has been an increase of +9% in the relative compositional contribution of SOA to $PM_{2.5}$ in BCN and +7% in MSY from 2009 to 2018.

2. Secondary sulfate was traced by SO_{4nss}^{2-} and NH_4^+, which were also present in the PMFs of both stations. This factor incorporates the formation of regional and long-range transported secondary sulfate aerosols, such as ammonium sulfate ($(NH_4)_2SO_4$)) (Pérez et al., 2016). Levels of SO_{4nss}^{2-} dramatically decreased in 2008 due to the implementation of the EU Directive for Large Combustion Plants (2001/80/EC) (European Parliament; Council of the European Union, 2001) in Spain, which reduced SO_2 emissions by 90% from a major European SO_2 emission source located 200 km southwest of Barcelona. All three PMF solutions attributed the same compounds to this source profile with slightly different percentages of SO_{4nss}^{2-}, NH_4^+, and OC. This resulted in similar concentrations being found in BCN, with 4.0 μgm^{-3} (26%) and 3.8 μgm^{-3} (24%) for the single and multisite solutions, respectively. However, a larger difference was found in MSY, with 2.00 μgm^{-3} (22%) and 2.77 μgm^{-3} (31%) for the single and multisite solutions, respectively. The difference in MSY was due to less SO_{4nss}^{2-} being attributed to this source, as a significant amount was instead attributed to the mixed marine and heavy oil source. The seasonal variability of secondary sulfate is characterized by higher concentrations in the summer due to a combination of low air mass renovation, enhanced photochemical activity and an increment of the summer mixing layer depth favoring the regional mixing of polluted air masses (Marmer and Langmann, 2005; Pérez et al., 2016; Querol et al., 2009a; Viana et al., 2014). Data from both stations also showed statistically significant decreases of −0.32 μgm^{-3} yr^{-1} (**; −6.9% yr^{-1}) and −0.15 μgm^{-3} yr^{-1} (*; −4.5% yr^{-1}) at BCN and MSY, respectively, which were very similar to those found for the single-site PMFs (−0.35 μgm^{-3} yr^{-1}; ***; −7.1% yr^{-1} for BCN; and −0.12 μgm^{-3} yr^{-1}; *; −4.9% yr^{-1} for MSY). Both stations also showed statistically significant trends during spring and summertime (−0.42 μgm^{-3} yr^{-1}; **; −7.6% yr^{-1} and −0.29 μgm^{-3} yr^{-1}; *; −4.6% yr^{-1} for BCN; and −0.18 μgm^{-3} yr^{-1}; *; −5.1% yr^{-1} and −0.16 μgm^{-3} yr^{-1}; *; −3.2% yr^{-1} for MSY, respectively).

3. (Aged) sea spray aerosol was a chemical profile dominated by Na and Mg, which also contained a significant contribution of SO_{4nss}^{2-}. This factor accounts for sea spray emissions. This source mostly included sea salt but also included a fraction of shipping-derived sulfate. This source was detected in the BCN PMF, with a similar source profile, which resulted in a similar average concentration of 2.1 μgm^{-3} (13%) being found in the BCN PMF compared to 1.8 μgm^{-3} (11%) in the multisite PMF. This source was not identified in the single-site MSY PMF as it was mixed with the heavy oil source. Comparing the concentrations between BCN and MSY in the multisite PMF, we obtained contributions of 1.8 μgm^{-3} (11%) and 1.0 μgm^{-3} (11%) for BCN and MSY, with a seasonal pattern of higher concentrations during summer. The contribution of SO_{4nss}^{2-} to this source resulted in a similar seasonal pattern to the one of secondary sulfate, which is characterized by increased levels during summer due to an increase enhanced photochemical activity, low air mass renovation, increment of the summer mixing layer depth favoring the regional mixing of polluted air masses, but also the possible higher summer contributions of secondary sulphate from DMS oxidation. During summer (Pérez et al., 2016; Querol et al., 2009a). However, only MSY showed

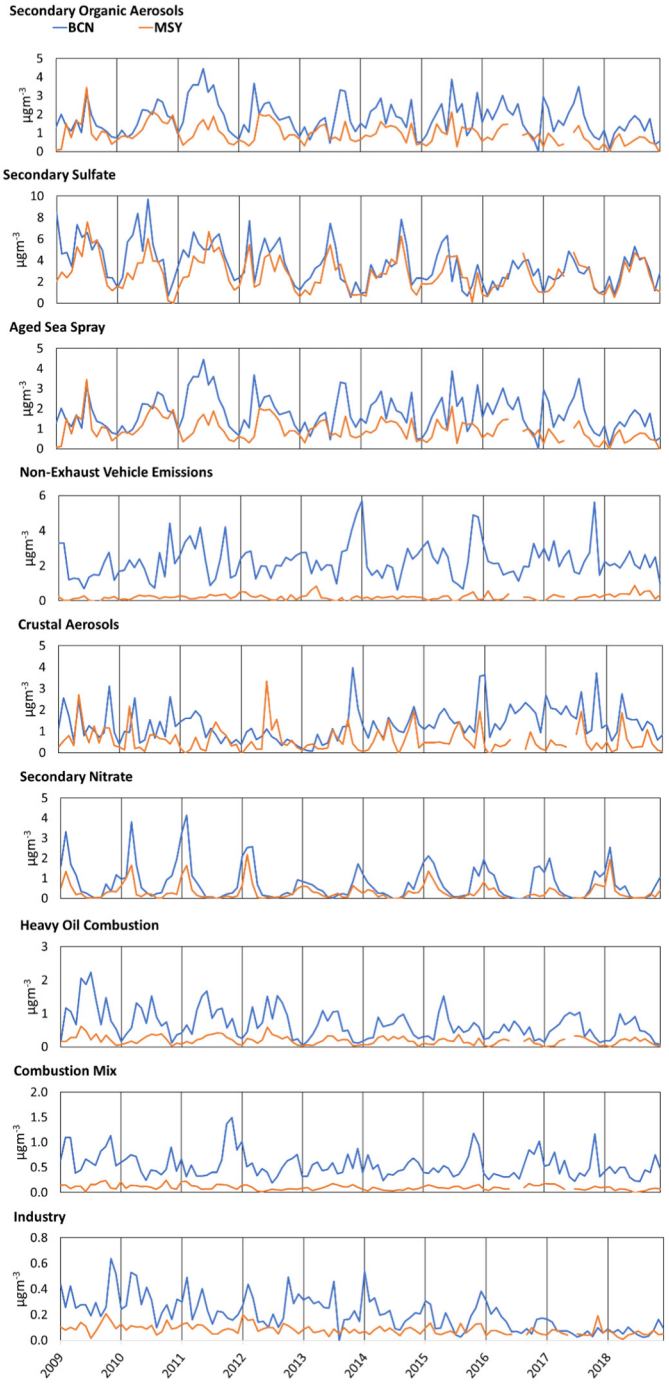

Fig. 3. Time series comparing the concentrations in μgm^{-3} of the nine identified major sources of the multisite PMF in BCN (blue) and MSY (orange).

a statistically significant decrease of -0.07 μgm^{-3} yr^{-1} (*; -5.2% yr^{-1}), exclusively significant during summertime (-0.08 μgm^{-3} yr^{-1}; *; -4.3% yr^{-1}).

4. Non-exhaust vehicle emissions were traced by Fe, Cu, and Sb. This factor accounts for non-exhaust vehicle emissions such as brake and tire wear (Amato et al., 2009a; Pérez et al., 2016), although a minor contribution from exhaust cannot be disregarded, as EC and OC were also attributed to this source. This source was detected in the PMF of the BCN station but not in the PMF for the MSY station, where these tracers were part of the mineral and combustion sources. The BCN and multisite source profiles were mostly similar, but the multisite PMF attributed 9% more EC (22% and 31% for BCN and the multisite, respectively) and 7% more OC (10% and 17%) to this source. These, in addition to some differences in trace elements, might explain the difference in concentrations found between the two PMF solutions, with 1.4 μgm^{-3} (8.7%) being attributed to this source on average during 2009–2018 in BCN and 2.2 μgm^{-3} (14%) in the multisite PMF. Nevertheless, this source had a higher contribution in BCN, where the average concentration was 2.2 μgm^{-3} (14%) compared to 0.2 μgm^{-3} (2.4%) in MSY. This was expected, as the BCN station is located in an urban area. The seasonal variance at both stations confirms this as well, with a clear seasonal variance in BCN with higher concentration in winter. But no seasonal variance was observed at the MSY station due to the distance from a traffic source. No statistically significant trend was found at any of the stations, with the exception of autumn in MSY, which showed a statistically significant increase of $+0.02$ μgm^{-3} yr^{-1} (+; +15% yr^{-1}). It is also notable that, at both stations, this was the only source whose concentrations have increased since 2009 (Fig. S3).
5. Mineral aerosols were traced by Al, Ca, Fe, Ti, Rb, and Sr, arising from both natural and anthropogenic dust sources (Amato et al., 2009b, 2016; Pandolfi et al., 2016; Pérez et al., 2016; Pey et al., 2013; Querol et al., 2001b, 2004a, 2009b). This source was detected in all PMF analyses. Comparing the concentrations of the single-site PMFs to the multisite PMF showed similar results, giving values of 1.7 μgm^{-3} (11%) and 1.3 μgm^{-3} (8.4%), respectively, for the single-site and multisite solutions in BCN and 1.0 μgm^{-3} (10%) and 0.6 μgm^{-3} (7.2%) for MSY. At both stations, the trends resembled those found in the mineral trend analysis described in Section 3.1. Neither PMF solution showed a statistically significant trend for either station. In MSY, a seasonal pattern with higher concentrations during summer was detected, but BCN did not show a significant seasonal pattern. The different seasonal patterns were a result of the different sources of mineral aerosols at both stations, with BCN being more affected by local emissions such as construction and traffic (Amato et al., 2009a, 2016; Pandolfi et al., 2016; Querol et al., 2001a) (Pandolfi et al., 2016). MSY on the other hand, is more affected by the regional mineral patterns that are known for having strong seasonal variability with higher levels in the summer due to the elevated dust resuspension of local and regional origin because of high convective dynamics and low rainfall, and an increase in African dust episodes frequency. Even though an attempt was made to remove the dust episode, its influence might still affect the results slightly because deposited African dust is continuously resuspeneded during days after the dust outbreak (N. Pérez et al., 2008a; Querol et al., 2009a).
6. Secondary nitrate was identified by NO_3^- and NH_4^+ and was previously detected at both stations. This factor accounts for the secondary NO_3^- formed in the atmosphere, mostly occurring as NH_4NO_3, but also as $CaNO_3$ and $NaNO_3$ in summer, associated with the coarse fraction (Amato et al., 2009a, 2016; Pandolfi et al., 2016; Pérez et al., 2016; Querol et al., 2001a). Secondary nitrate showed a strong seasonal pattern, with relatively high concentrations in winter and very low (<0.05 μgm^{-3}) concentrations during summertime at both stations due to the higher ambient temperatures favoring volatilization of NH_4NO_3 into HNO_3 and NH_3 in the hot Barcelona summers (Querol et al., 2001a, 2009a). The source profiles were similar between the three PMFs, with only the BCN PMF mapping 6.8% OC onto this source, compared to the 2.9 and 2.2% of the MSY and multisite PMFs. This is probably the cause of the difference seen in concentrations between the single-site and multisite PMFs of BCN, with 1.5 μgm^{-3} (9.6%) attributed to this source in the single-site PMF and 0.8 μgm^{-3} (4.9%) in the multisite PMF. All three PMF solutions also showed a contribution of K from this source, which again might indicate a minor contribution of biomass burning being mixed in this source (Brines et al., 2019). The mostly anthropogenic source of nitrate is seen in the comparison between the two

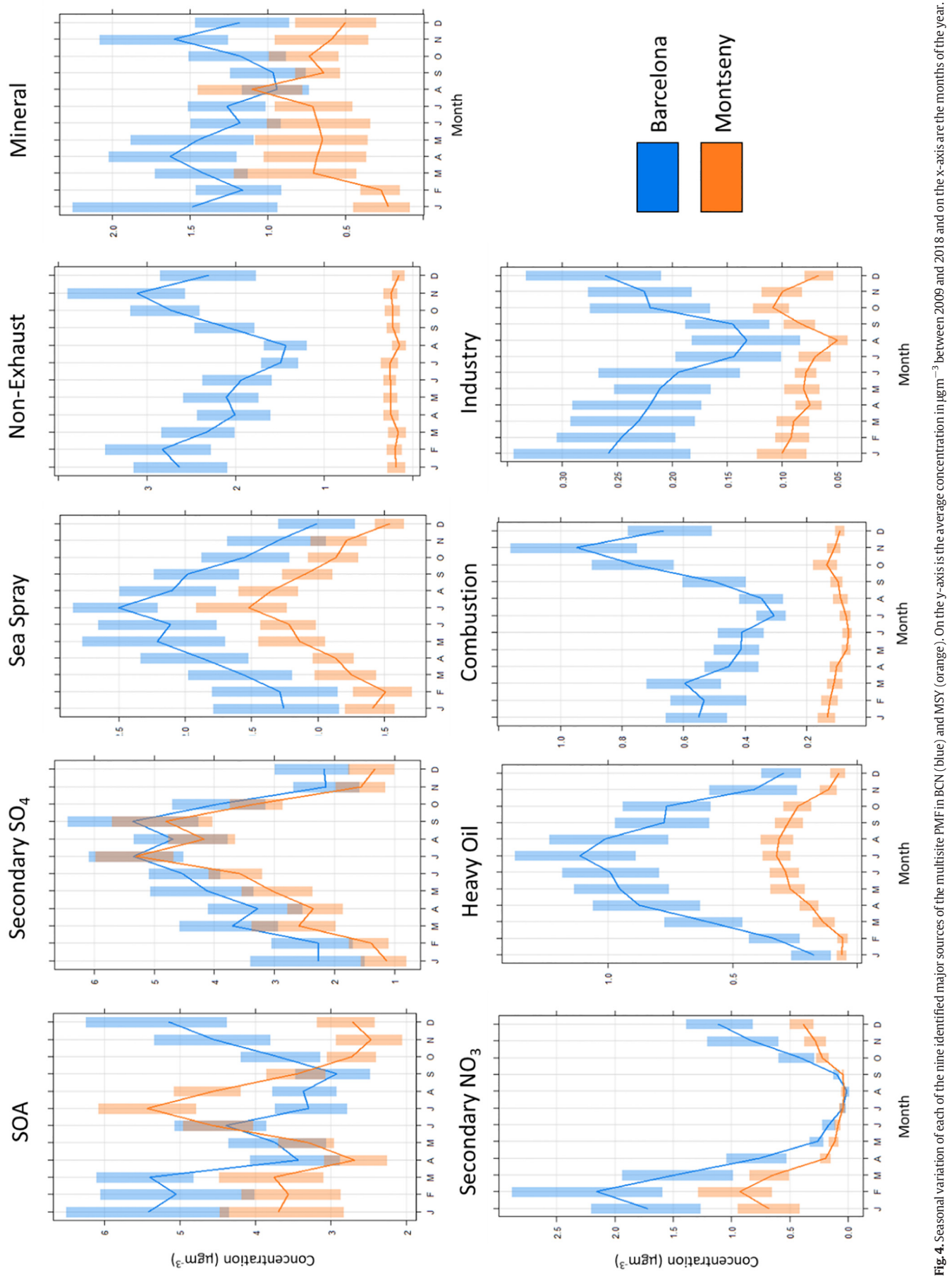

Fig. 4. Seasonal variation of each of the nine identified major sources of the multisite PMF in BCN (blue) and MSY (orange). On the y-axis is the average concentration in μgm^{-3} between 2009 and 2018 and on the x-axis are the months of the year.

stations: concentrations were 2.5 times higher in BCN (0.8 μgm^{-3} (4.9%)) than in MSY (0.3 μgm^{-3} (3.5%)). Of the two sites, only BCN showed a statistically significant decrease of -0.04 μgm^{-3} yr^{-1} (+; -4.6% yr^{-1}) on an annual basis, which was only detected during springtime with a magnitude of -0.10 μgm^{-3} yr^{-1} (+; -9.3% yr^{-1}).

7. Heavy oil was traced by V and Ni, which were detected only in BCN, and mixed with sea spray in MSY. Currently, in and around Barcelona, this factor mostly originates from shipping emissions (Amato et al., 2009a, 2016; Pandolfi et al., 2020; Pérez et al., 2016). This clear seasonal variation is a result of an seasonal increase of i) the higher summer sea breeze frequency, but also to ii) the increase of touristic cruises, other passenger vessels, small vessels, and container ships (Jalkanen et al., 2016; Pérez et al., 2016; Pey et al., 2013). The BCN single-site and multisite PMFs produced similar source profiles for this source, resulting in similar concentrations of 0.7 μgm^{-3} (4.6% and 4.7%, respectively for the single-site and multisite) being attributed to this source. Comparing the concentrations of the two stations showed that the contributions were significantly higher in BCN, with an average of 0.7 μgm^{-3} (4.7%), compared to 0.2 μgm^{-3} (2.2%) in MSY. A statistically significant decreasing trend could be observed at both sites with values of -0.05 μgm^{-3} yr^{-1} (+; -6.3% yr^{-1}) in BCN and -0.02 μgm^{-3} yr^{-1} (*; -6.5% yr^{-1}) in MSY, consistent over all seasons (from -0.05 to -0.09 μgm^{-3} yr^{-1}; * to ***; -5.1 to -8.1% yr^{-1} for spring, summer, and autumn in BCN; and from -0.01 to -0.02 μgm^{-3} yr^{-1}; + to *; -4.1 to -9.6% yr^{-1} for summer, autumn, and winter in MSY).
8. Mixed combustion was traced by EC and Sb. This source was detected in both single-site PMFs as traffic exhaust in BCN and as the mixed combustion source in MSY. The differences between the single-site PMFs and the multisite PMF were quite significant here, with all three PMFs attributing different contributions of EC and OC to this source (Fig. 2). The low levels of OC in the multisite PMF probably mean that this source only includes primary OA from traffic in the multisite PMF. Thus, SOA from traffic is included in the secondary organic aerosols source in the multisite analysis and not in this combustion source. The seasonal variance of both stations portray higher concentrations during the winter, and lower during the summer caused by increased biomass burning (Minguillón et al., 2011), higher anthropogenic emission rates and lower atmospheric dispersive conditions (Viana et al., 2006). Much higher concentrations were found in BCN compared to MSY (0.6 μgm^{-3} (3.6%) and 0.1 μgm^{-3} (1.1%), respectively). This was expected due to the proximity of various anthropogenic sources to BCN compared to MSY. Nevertheless, both stations showed a statistically significant decrease of -0.02 μgm^{-3} yr^{-1} (+; -3.3% yr^{-1}) and -3.4×10^{-3} μgm^{-3} yr^{-1} (+; -2.8% yr^{-1}) respectively in BCN and MSY, and also showed a statistically significant decrease during summer (-0.02 μgm^{-3} yr^{-1}; +; -5.0% yr^{-1} and -0.01 μgm^{-3} yr^{-1}; *; -5.2% yr^{-1} for BCN and MSY). BCN also had a significant decrease during winter (-0.02 μgm^{-3} yr^{-1}; *; -3.2% yr^{-1}). The single-site PMF of BCN only showed a trend during summertime, of -0.13 μgm^{-3} yr^{-1} (+; -3.5% yr^{-1}), and MSY had a statistically significant decrease of -0.02 μgm^{-3} yr^{-1} (+; -1.8% yr^{-1}) on an interannual basis, but no other trends were detected during any particular season.
9. Industry was traced by Mn, Zn, Cd, and Pb. This source represents a mixture of common tracers in BCN from industrial activities, such as smelters and cement kilns (Amato et al., 2009b; Cusack et al., 2012; Pandolfi et al., 2016; Pérez et al., 2016; Querol et al., 2007, 2014) and emissions from various industries on a regional scale (Cusack et al., 2012; Pandolfi et al., 2016). The source profiles of the multisite and BCN PMFs seemed consistent with this source, with a significant difference from MSY: the MSY PMF also attributed Co, Ni, and much more Cu to this source, among other tracers (Fig. 2). The difference between the three PMF solutions is also reflected in the difference between the single-site and multisite PMFs, with 0.2 μgm^{-3} (1.4%) and 0.3 μgm^{-3} (1.8%) attributed to this source in the BCN PMF and the BCN multisite PMF, respectively, and 0.5 (5.3%) and 0.1 μgm^{-3} (0.94%) in the MSY PMF and the MSY multisite PMF, respectively. This indicates that in the multisite PMF, this source is mostly from metallurgy, while regional industry was detected in the MSY single-site PMF. In 2009, the concentrations were much higher in BCN compared to MSY (0.3 μgm^{-3} (1.8%) compared to 0.1 μgm^{-3} (1.1%), respectively), but the concentrations of this source steadily decreased over time in BCN, with a steep decrease starting in 2014, while MSY showed a constant decrease. At the end of 2018, the concentrations of this source were very similar (0.1 μgm^{-3} (0.6%) in BCN and MSY. This was also observed in the statistically significant decreases detected in both stations, with values of -0.03 μgm^{-3} yr^{-1} (***; -7.5% yr^{-1}) and -0.01 μgm^{-3} yr^{-1} (***; -5.8% yr^{-1}), respectively, for BCN and MSY. This was measured over all seasons (except winter in MSY), with varying significance (from -0.03 to -0.04 μgm^{-3} yr^{-1}; * to ***; 6.0 to 9.8% yr^{-1} in BCN; and -2.9×10^{-3} to -0.01 μgm^{-3} yr^{-1}; + to *; -3.6 to 7.7% yr^{-1} in MSY). A seasonal pattern could be observed at both stations, with concentrations relatively higher during the winter compared to the other seasons. The increased concentrations during the cold months of the year are a result of prevalent stagnant atmospheric conditions in which local pollutants dominate (Moreno et al., 2011; Pérez et al., 2016; Pey et al., 2010). The rate of decrease strengthened sharply since 2013 on a per-year basis, following the recovery from the financial crisis (see discussion).

In order to confirm the identification of an SOA source, a correlation study was performed between the ACSM measurements of OOA and the filter sample PMF source contributions over a year-long period (Fig. 5). Using the daily averaged values, a relatively good year-round correlation was obtained for BCN, with a slope of 0.73 for the Filter-PMF/OOA-ACSM relationship with the intercept set to 0 ($R^2 = 0.85$). The disaggregation of the data into summer and winter revealed a higher correlation during summer (when SOA increased markedly), with a slope of 0.94 ($R^2 = 0.92$), and a slope of 0.58 ($R^2 = 0.87$) during winter. Similar results were found in MSY, with a year-round slope of 0.67 ($R^2 = 0.77$), and slopes of 0.84 ($R^2 = 0.92$) during summertime and 0.15 ($R^2 = 0.78$) during wintertime. All correlations had a p-value < 0.01. The divergence between the two seasons can have a variety of reasons. First, the PMF solution of the ACSM differs between the two seasons, where during summer two secondary OA factors were found (LO-OOA and MO-OOA), but during winter a single OOA factor was extracted, but also included the presence of a biomass burning factor (Via et al., 2021). Furthermore, the difference between the two methods (Fig. S4) could stem from the two different measuring principles, as different PM size cutoffs (PM_1 in ACSM and $PM_{2.5}$ in filters), measuring principles, and PMF analyses were applied. However, the high correlations overall indicated that the source was well identified.

4. Discussion

Combining the results of the Theil–Sen trend estimation and PMF source contribution analyses while comparing the two stations allowed determination of the trends in $PM_{2.5}$ and source contributions in NE Spain. The multisite PMF contributed additional information to the PMF analysis of the stations. First, the multisite PMF allowed us to identify sources at both stations that could not previously be identified in the single station PMFs, such as the aged sea spray aerosols and heavy oil combustion in MSY and SOA in BCN. Furthermore, the multisite PMF allowed us to make a direct comparison between the stations (Fig. 3). The fact that similar chemical profiles were found in the multisite PMF compared to the single station PMFs strengthens the reliability of the multisite PMF approach. However, the multisite PMF is not a perfect solution: while the seven largest sources were distinguished and agreed relatively well with the single-site PMFs, two sources (mixed combustion and industry) showed significant differences. In the case of mixed

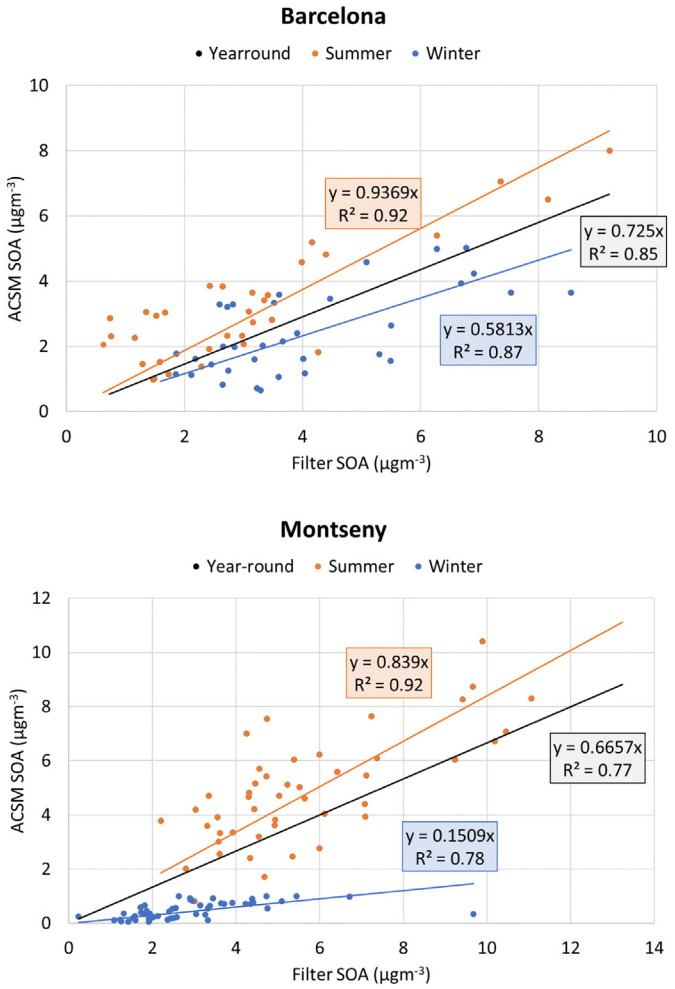

Fig. 5. The correlations between the $PM_{2.5}$ filter SOA concentrations and the PM_1 OOA ACSM concentrations in BCN in 2017–2018 (top) and in MSY in 2012–2013 (bottom). Year-long correlations (black) and the summertime (orange) and wintertime (blue) correlations are shown for each location.

combustion, this was due to the attribution of OC to the SOA source in BCN and the mixed combustion being separated in MSY, allowing for a better solution. However, in the multisite PMF, the industry source was dominated by the metallurgy industry (as seen in the source profile, Fig. 2), which removed the regional industry source of MSY in the multisite PMF. Nevertheless, due to the many advantages of the multisite PMF and the verification by the single-site PMFs, only the multisite PMF will be discussed in the following section, where we discuss the results of the different analyses to interpret the causes of possible trends or the absence of trends.

4.1. Trends in $PM_{2.5}$ over different periods

Previous long-term trend analyses were not available using the data from our monitoring station in BCN due to the relocation that occurred in 2008, but various trend analyses were performed for the MSY data. Cusack et al. (2012) evaluated the $PM_{2.5}$ gravimetric mass concentrations and the chemical species during the period 2002–2010 in MSY, while Pandolfi et al. (2016) performed a follow-up study at the same station, with the addition of a PMF analysis between 2002 and 2014. Decreases of -0.7 µgm^{-3} yr^{-1} (**) and -0.3 µgm^{-3} yr^{-1} (*) were found by Cusack et al. (2012) and Pandolfi et al. (2016), respectively. The 50% reduction in slope between the two research periods was attributed to a large increase in concentrations in 2012, which was outside the observation period of Cusack et al. (2012). Pandolfi et al. (2016) attributed this increase to a rise in organic matter during 2012, and while we do not disregard this conclusion, as will be discussed later, we found a second possible source of this $PM_{2.5}$ peak in our analysis. While we did not use the gravimetric mass method to calculate $PM_{2.5}$, a large difference was measured in 2012 between the results of the gravimetric mass method and the sum of the chemical speciation, showing the significant influence of the unaccounted water-driven mass when using the gravimetric method. Due to the difference in method, no comparison can be made with previously published results.

4.2. OA & EC, and their various associated PM source contributions

The relative contribution of the OA to $PM_{2.5}$ increased from 2009 to 2018 by 12% and 9% in BCN and MSY, respectively. Together with EC, it accounted for almost 50% of the composition by 2018, signifying its importance in $PM_{2.5}$. Previous studies reported decreases in OC and EC between 2002 and 2010 at the MSY station (Cusack et al., 2012), with a statistically significant trend of OC reaching -0.18 µgm^{-3} yr^{-1}, seen across all seasons, with a seasonal pattern for OC that showed higher concentrations during the summer. This was caused by the lower renewal of the atmospheric air masses at the regional scale in summer (L. Pérez et al., 2008b; Rodríguez et al., 2002), higher biogenic emissions of VOCs (Seco et al., 2011), and higher secondary aerosol formation ratios due to enhanced summer photochemistry. Meanwhile, Pandolfi et al. (2016) did not find a statistically significant trend at MSY between 2004 and 2014, which they attributed to the relevant contribution from biogenic SOA to regional background $PM_{2.5}$. During our study period, no statistically significant trend was found in BCN for OA, SOA, or EC. The lack of trend was partially driven by the peaks in 2011 and 2015, which were detected in both OA, SOA, and EC. The 2009–2018 trends at MSY were consistent with the findings of Pandolfi et al. (2016), as no significant trend was found for OA, largely due to the increase in concentrations in 2011 and 2012. Whereas the peaks were seen in all constituents in BCN, this was not the case in MSY. While OA showed higher concentrations in both 2011 and 2012, EC only showed a peak in 2011 and SOA in 2012, which means that these peaks have different origins (combustion-influenced in 2011 and SOA-influenced in 2012). The SOA peak in 2012 contributes to the hypothesis stated by Pandolfi et al. (2016) that the $PM_{2.5}$ peak in 2012 originated from an increase in biogenic SOA. The seasonal variability between the stations also differed (Fig. 4). In BCN, EC showed a seasonal pattern with higher concentrations in winter; this pattern was absent in MSY. By contrast, in MSY, OA showed higher concentrations during summer due to the increase in biogenic SOA at this station (Cusack et al., 2012; Pandolfi et al., 2016) which was not seen in BCN.

The three major identified OC- and EC-contributing PMF sources were SOA, mixed combustion, and non-exhaust vehicle emissions. Mixed combustion was the only source of these three that showed a statistically significant decrease at both stations. In BCN between 2003 and 2012, Pandolfi et al. (2016) reported a marked decrease of this contribution, with EC being reduced by nearly 50% due in part to the impact of local air quality measures, but especially due to the EURO vehicle emission standards for PM emission by diesel vehicles. This decrease has continued since 2009, albeit not as steeply as between 2003 and 2012. Finally, a cooking source has not been identified in this study, indicating that the PM chemical composition dataset does not contain enough information to detect such a source, although it has been identified and quantified by previous studies using aerosol mass spectrometers (Escudero et al., 2015; Mohr et al., 2012; Via et al., 2021).

4.3. Mineral aerosols

Crustal aerosols contain both natural and anthropogenic contributions and reached 11% and 10% of the $PM_{2.5}$ in BCN and MSY, respectively. Previous studies of MSY $PM_{2.5}$ composition showed a decreasing trend from 2002 to 2012 (Cusack et al., 2012) and from 2001 to 2012 (Querol et al., 2014). These studies included samples from days with African

dust outbreaks, whose frequency and intensity over NE Spain were driven by the negative North Atlantic Oscillation index (Pey et al., 2013). Especially during 2008–2012, this was quite negative, leading to lower PM contributions from the Saharan dust episodes. To remove the influence of the Saharan dust episodes, days with reported intrusions were removed from the datasets in the present study. This resulted in a significant difference between annual variations of the crustal load trends at MSY, as seen in Fig. S5.

Another source of crustal material arises from construction and demolition emissions. Pandolfi et al. (2016) elaborated on this, explaining that the observed decrease originated from the economic recession of 2008. This hypothesis was confirmed by the observations in BCN, which has traffic and construction as more predominant sources of crustal material, compared to MSY, which is located far away from these sources. BCN did not show a statistically significant trend because the concentration decreased from 2009 until 2012, after which it increased again until 2016 (Fig. S6). From 2016 onward, the concentrations decreased again. The decrease from 2009 to 2012 is consistent with observations of the effects of decreased construction and demolition associated with the economic recession, reported by prior studies. Since 2012, the recovery from the recession probably caused an increase in emissions from this industrial sector. For example, in a dataset of the number of home constructions started in Barcelona from 2000 to 2020, a significant decrease is observed from 2008 to 2012, with a reduction of 94%. However, since 2012, the number of constructions has increased steadily every year. By 2018, the number of constructions had increased by 93% compared to 2012 (Barcelona City Council, 2020, Fig. S7). Furthermore, daily vehicle counts from the four busiest streets in Barcelona showed similar behavior, with a decrease until 2012–2013, after which the volume slowly increased again (Barcelona City Council, 2016, 2010, 2005; Fig. S8). As noted above, MSY, with the NAF episode days removed, showed neither a 2009–2018 significant trend for crustal aerosols nor the same pattern as in BCN due to its distance from construction and traffic sources.

4.4. Heavy oil combustion

Heavy oil combustion was traced by V and Ni, which contributed 4.7% to $PM_{2.5}$ in BCN and 2.2% in MSY. Previous papers also indicated a relation with SO_4^{2-} which the PMF did not detect (Pandolfi et al., 2016; Pérez et al., 2016; Viana et al., 2014). V, Ni, and SO_4^{2-} (the latter as both primary PM and secondary PM from SO_2 emissions) are all constituents of heavy oil combustion emissions, which originate from two main sources in BCN: industry and shipping emissions. However, various emission abatement strategies have been implemented related to heavy oil over the last decade to improve air quality. Regional air quality plans phased out fuel oil, replaced by natural gas, for power generation around BCN in 2007 (Cusack et al., 2012; Pandolfi et al., 2016; Querol et al., 2014), while at the same time the International Maritime Organization (IMO)/MARPOL and the EU set limits on S content in the fuel emissions from ships (Organization International Maritime, 2011; European Parliament; Council of the European Union, 2005). With energy production removed as a source of heavy oil combustion before the study period and S emissions from shipping emissions being limited around BCN, only V and Ni remained as tracers for shipping emissions.

Prior studies reported a large decrease in levels of SO_{4nss}^{2-}, V, and Ni in both BCN and MSY (Pandolfi et al., 2016; Querol et al., 2014) related to policy actions affecting heavy oil combustion (for all three tracers) and the implementation in 2008 of the Large Combustion Plants Directive (for SO_{4nss}^{2-}). This decreasing trend continued between 2009 and 2018, with a statistically significant decrease at both stations (-0.05 μgm^{-3} yr^{-1}; +; and -0.01 μgm^{-3} yr^{-1}; *; respectively). Of the two metals, only V showed a statistically significant decrease at both stations (BCN: -6.2% yr^{-1}; **; and MSY: -5.4% yr^{-1}; **). The lack of a trend for Ni might indicate that it has an additional industrial source. When comparing the trends in the heavy oil combustion source of the multisite PMF, a similar decrease can be observed, of -6.3% yr^{-1} in BCN and -6.5% yr^{-1} in MSY.

4.5. Secondary inorganic aerosol

The SIA factor is the second major contributor to $PM_{2.5}$, with respective values of 37 and 43% in BCN and MSY. Both stations measured a significant decrease (-0.23 μgm^{-3} yr^{-1}; *; and -0.10 μgm^{-3} yr^{-1}; *; in BCN and MSY). At both stations, the majority of SO_4^{2-}, NO_3^-, and NH_4^+ were attributed to the formation of secondary $(NH_4)_2SO_4$ and NH_4NO_3, with a minor amount of SO_4^{2-} attributed to the heavy oil/sea spray sources as mentioned earlier. While in the atmosphere, SO_4^{2-} and NO_3^- might also occur as $CaSO_4$, $MgSO_4$, Na_2SO_4, $Ca(NO_3)_2$, $Mg(NO_3)_2$, and $NaNO_3$, which occur mostly in the coarse PM fractions and not in $PM_{2.5}$ (Pérez et al., 2016).

Atmospheric NH_4^+ mostly originates from agricultural and farming ammonia (NH_3) emissions but also from urban sources (Reche et al., 2015; Sutton et al., 2013). Van Damme et al. (2018) found NE Spain to be a major European NH_3 hotspot due to agricultural and farming emissions. Furthermore, high NH_3 urban emissions were found in Barcelona (Pandolfi et al., 2012; Reche et al., 2015), where much higher concentrations were measured compared to other Spanish cities. The high NH_3 concentrations recorded in the study area were very relevant in reducing the $PM_{2.5}$, as even if SO_x and NO_x emissions were reduced, the high levels of NH_3 would still favor the formation of SIA. In BCN and MSY, a slight statistically significant decrease in NH_4^+ was detected, with a value of -2.2% yr^{-1} in MSY and a much greater value of -5.9% yr^{-1} in BCN, in both cases mostly found in spring.

Secondary sulfate aerosols provided the second highest $PM_{2.5}$ contributions in the PMF source apportionment analyses, accounting for 24% in BCN and 31% in MSY. SO_{4nss}^{2-} showed a significant decrease at both stations (-5.1% yr^{-1}; *** in BCN; and -4.0% yr^{-1}; ** in MSY), with a clear seasonal pattern observed, characterized by the highest concentrations occurring in summer. This is due to low oxidation ratios of SO_2 during winter of <1% h^{-1} compared to 6% h^{-1} in the summer in the Mediterranean area (Querol et al., 1999a, 1999b). This indicates that the various abatement measures in shipping, industry, and power generation have worked efficiently both locally and regionally, with rates of decrease that were half those for 2004–2014 (Pandolfi et al., 2016) due to the strong effect of the European Large Combustion Plants and Industrial Emission Directives and other European and regional measures abating SO_2 emissions prior to 2009. Thus, in 2016, the United Nations Economic Commission for Europe (UNECE) reported that only a further 20% reduction in SO_2 emissions could be achieved through measures in industry, residential and commercial heating, and reduced agricultural waste burning (Pandolfi et al., 2016; UNECE, 2016). This was also seen in the flattening of the decreasing trend of SO_{4nss}^{2-} (Appendix A).

The secondary nitrate PMF source showed a seasonal pattern, with concentrations close to the detection limit during summer and growing during winter periods. This is due to the low thermal stability of NO_3^- under typical hot summer conditions (Querol et al., 2001a). A statistically significant decreasing trend was only detected in BCN, which showed a continuous decrease with the exception of a sharp increase in 2015. NO_x, the precursor to NO_3^-, has a mostly anthropogenic origin, originating mainly from traffic in BCN but also from power generation, industry, and the domestic sector (Pandolfi et al., 2020, 2016). The various initiatives to reduce NO_x emissions in BCN had a significant impact in abating NO_x, decreasing NO concentrations by -28.8% and NO_2 by -20.6% between 2005 and 2017 (Massagué et al., 2019; Pandolfi et al., 2016). EURO 6 standards for vehicle emission and the economic recession also reduced traffic flows and industrial emissions in 2008–2013. Since 2013–2015, urban traffic counts have increased again. This might explain the increased concentrations observed since that time (Fig. S8). While this trend was observed in BCN, MSY lacked a statistically significant trend after 2009. Using the multisite PMF analysis to compare the concentrations between the two stations, it was

observed that, on average, the concentrations were almost 2.5 times higher in BCN compared to MSY (0.8 μgm^{-3} vs. 0.3 μgm^{-3}). This was also detected in the different contributions in the PMFs, contributing 4.9% of $PM_{2.5}$ to secondary nitrate in BCN but only 3.5% in MSY. While SO_4^{2-} has a more regional origin, showing similar concentrations in BCN and MSY, urban NO_3^- is very relevant, with much higher levels recorded in BCN.

4.6. Aged sea spray aerosols

In BCN, no statistically significant trends were found in the sea spray source. In MSY, this source showed a statistically significant decrease over the period of −0.07 μgm^{-3} yr^{-1} (*; −5.2% yr^{-1}), mostly due to a huge reduction in 2017. This is a surprising observation, as sea spray aerosols are not expected to vary interannually. This decrease was also seen in Na_{ss} during autumn and winter when a statistically significant decrease was observed. This decrease could probably be a limitation of the method applied, as Cl^- could not be used due to the unreliable data, and Na_{ss} was calculated indirectly, as were the other constituents (K_{ss}, Mg_{ss}, Ca_{ss}, and SO_{4ss}^{2-}). A second explanation could be the anthropogenic load of the aged sea salt source from shipping traffic over the Mediterranean Sea. This trend was only seen in the summertime yearly average of the seasonal PMF (−0.08 μgm^{-3} yr^{-1}; *; −4.3% yr^{-1}). Both stations did show a seasonal pattern with lower concentrations during winter and higher concentrations during the summer due to a strong influence from sea breezes (Querol et al., 2008). Concentrations in BCN of this source were almost twice as high as in MSY (1.8 and 1.0 μgm^{-3}, respectively), most likely due to the proximity of BCN to the sea.

4.7. Metallurgy

The metallurgy industry has been indicated as the main industrial sector contributing to $PM_{2.5}$ in BCN and MSY (Amato et al., 2009a, 2016; Cusack et al., 2012; Pandolfi et al., 2016; Pérez et al., 2016). Both BCN and MSY showed a very high statistically significant decrease (−7.2% yr^{-1}; ***; and −5.8% yr^{-1}; ***) in this source. The concentrations were about 2.5 times higher in BCN compared to MSY when comparing the metallurgy source due to the proximity of smelters to BCN. Although the main PM emission abatement from the smelters around Barcelona occurred during the implementation of the Industrial Emissions Directive (European Parliament; Council of the European Union, 2008; Pandolfi et al., 2016), just before our study period, our results show that there was still a decrease in metallurgy PM contributions in 2009–2018, probably due to the 2008–2013 financial crisis and the regionally implemented measures. By 2018, the contributions of the industry source were similar in BCN and MSY.

4.8. Biomass burning

Biomass burning was not identified as a source in either PMF because we did not use organic tracers. Previous research, using these together with inorganic tracers, detected and quantified the biomass burning contribution to $PM_{2.5}$ (Amato et al., 2016; Reche et al., 2012; Viana et al., 2013) or PM_1 (Brines et al., 2019) in BCN. These studies concluded that during winter, about 7–8% of the $PM_{2.5}$ was contributed by biomass burning (Reche et al., 2012; Viana et al., 2013). Viana et al. (2013) determined that contributions of K-related aerosols from regional biomass burning were mixed in a source of regional-scale secondary aerosols during a winter campaign in 2011. Amato et al. (2016) concluded that the biomass source contribution to the annual $PM_{2.5}$ average was <2.5%. Brines et al. (2019) confirmed this by identifying a biomass burning source for PM_1 in BCN, which was mixed with secondary nitrate. This can also be observed in the source profiles of this study, with the two SOA sources of the MSY PMF and multisite PMF each contributing about 20% of K to this source. Comparing the MSY and multisite source profiles, various minerals were excluded, with the exception of K. This could indicate that biomass burning might be partially included in this source, especially since a minor contribution of EC was included in the multisite PMF. Furthermore, the source profiles of all three PMF solutions contributed 10–15% of K to the secondary nitrate source, which might indicate regionally transported biomass burning emissions were also partially included in this source. In BCN, the K_{bb} tracer showed a decreasing trend on an annual basis, with higher concentrations during the summer compared to the winter. This is an atypical seasonal pattern for biomass burning, indicating a low impact of domestic biomass burning and a higher impact from regional agricultural burns and forest fires. Other trends, with the exception of autumn in BCN, were absent at both stations.

5. Conclusions

2009−2018 time-series analyses of the major and minor components and source contributions of $PM_{2.5}$ in NE Spain were obtained from a set of twin stations, an urban background station in Barcelona (BCN) and a rural background station in Montseny (MSY). To compare the source profiles and source contributions between the two stations, a multisite PMF analysis was performed. This PMF analysis successfully identified 9 sources and allowed us to determine the source contribution of SOA in BCN and to distinguish (aged) sea spray aerosols and heavy oil combustion in MSY while losing the regional industry source from the MSY station. While nine sources were successfully identified, this solution was not able to identify a cooking source or a biomass burning source, which were previously detected in the same area using ACSM or offline analysis with organic speciation, indicating the limitations of the dataset.

Previously reported decreases in $PM_{2.5}$ were found to have continued at both stations during the 2009−2018 period, with rates of −0.34 and −0.24 μgm^{-3} yr^{-1} in BCN and MSY, respectively, corresponding to decreases of −2.8% yr^{-1} and −3.3% yr^{-1}. These decreases were driven by a continuous statistically significant decrease source contributions from in heavy oil combustion (−6.9 and −6.5% yr^{-1} for BCN and MSY, respectively), mixed combustion (−3.3 and −2.8% yr^{-1}), and the industry source (−7.5 and −5.8% yr^{-1}) at both stations. These source contributions are all related to anthropogenic emissions, which implies the continuing success of pollution abatement strategies in NE Spain on both an urban and regional scale over time. The various abatement strategies for sulfate-bearing compounds also resulted in a significant decrease in the secondary sulfate source (−6.9 and −4.5% yr^{-1}) at both stations. Furthermore, there was also a statistically significant decrease in secondary nitrate (−4.6% yr^{-1}) in BCN, which is related to the abatement of anthropogenic emissions as well and was mostly driven by a continuous decrease in NO_x in the urban area of BCN. Meanwhile, in MSY, a statistically significant decrease in SOA was observed (−1.4% yr^{-1}), although this decrease was the smallest of all those observed. These trends were also reflected in the statistically significant trends of the various pollutants at both stations, with both sites showing decreasing trends in SIA and all constituents (with the exception of NO_3^- in MSY), the sum of the trace elements, and V. Differences between the stations included a decrease in K_{bb} and NO_3^- in BCN, and in various minerals (Al_2O_3, Na_2O_{dust}, K_2O_{dust}, TiO_2) and EC in MSY.

These decreasing trends have affected the relative composition of $PM_{2.5}$ particles at both stations. In 2009, SIA contributed with the largest fraction to the annual average $PM_{2.5}$ in BCN, accounting for 39%, while OA, the second most relevant contributor, accounted for 30%. By 2018 OA was the first contributor, with 41%, followed by SIA with 34%. This increase in OA was mostly of secondary origin, with an increase of 12% from 2009 to 2018 (+0.65% yr^{-1}), while EC and NO_3^- did not change in relative contribution. In MSY, OA already constituted the largest group of $PM_{2.5}$ in 2009 with a contribution of 41%, but this increased to 50% in 2018, with an SOA contribution of 40% of the total $PM_{2.5}$ in 2018. The relative contribution from SIA did not change much, as the

small decreases in SO_{4nss}^{2-} and NH_4^+ were compensated by an increase in relative NO_3^-. This was also supported by the source contributions, with SOA as the largest source at both stations, accounting for 30% in BCN and 44% in MSY by 2018, an increase of 9% in BCN and 7% in MSY.

The increase in the relative contribution of OA in both urban and rural $PM_{2.5}$ might indicate that even though bulk concentrations of $PM_{2.5}$ have decreased, its composition has markedly changed as probably varied the toxicological patterns, as OA (relatively increasing) might have a different oxidative potential to SIA (relitavely decreasing). A follow-up study that includes more detailed speciation of the OA fraction is therefore recommended, as this is now the largest constituent of $PM_{2.5}$, as well as studies to evaluate the oxidative potential of the newer $PM_{2.5}$ composition. These results are also relevant for air quality policy and measures to further continuing abating $PM_{2.5}$, indicating a need to better evaluate urban compositions and levels of volatile organic species producing SOA and O_3 in order to devise cost-efficient measures to reduce pollution.

CRediT authorship contribution statement

Marten in 't Veld: Software, Formal analysis, Investigation, Writing – original draft, Writing – review & editing, Visualization. **Andres Alastuey:** Investigation, Validation. **Marco Pandolfi:** Software, Validation, Formal analysis. **Fulvio Amato:** Validation. **Noemi Pérez:** Investigation, Validation. **Cristina Reche:** Investigation, Validation. **Marta Via:** Resources. **María Cruz Minguillón:** Resources. **Miguel Escudero:** Validation. **Xavier Querol:** Conceptualization, Methodology, Validation, Investigation, Writing – review & editing, Visualization, Supervision, Project administration, Funding acquisition.

Declaration of competing interest

The authors declare that they have no known competing financial interests or personal relationships that could have appeared to influence the work reported in this paper.

Acknowledgements

The present work was supported by the Spanish Ministerio para la Transición Ecológica (17CAES010); the "Agencia Estatal de Investigación" from the Spanish Ministry of Science, Innovation and Universities, and FEDER funds under the projects CAIAC (PID2019-108990RB-I00) and HOUSE (CGL2016-78594-R); and the Generalitat de Catalunya (AGAUR 2017 SGR41). We would like to thank the Direcció General de Territory i Sostenibilitat from the Generalitat de Catalunya for providing us with air quality data.

Appendix A. Supplementary data

Supplementary data to this article can be found online at https://doi.org/10.1016/j.scitotenv.2021.148728.

References

Amato, F., Pandolfi, M., Escrig, A., Querol, X., Alastuey, A., Pey, J., Perez, N., Hopke, P.K., 2009a. Quantifying road dust resuspension in urban environment by multilinear engine: a comparison with PMF2. Atmos. Environ. 43, 2770–2780. https://doi.org/10.1016/j.atmosenv.2009.02.039.

Amato, F., Pandolfi, M., Viana, M., Querol, X., Alastuey, A., Moreno, T., 2009b. Spatial and chemical patterns of PM10 in road dust deposited in urban environment. Atmos. Environ. 43, 1650–1659. https://doi.org/10.1016/j.atmosenv.2008.12.009.

Amato, F., Alastuey, A., Karanasiou, A., Lucarelli, F., Nava, S., Calzolai, G., Severi, M., Becagli, S., Gianelle, V.L., Colombi, C., Alves, C., Custódio, D., Nunes, T., Cerqueira, M., Pio, C., Eleftheriadis, K., Diapouli, E., Reche, C., Minguillón, M.C., Manousakas, M.I., Maggos, T., Vratolis, S., Harrison, R.M., Querol, X., 2016. AIRUSE-LIFE+: a harmonized PM speciation and source apportionment in five southern European cities. Atmos. Chem. Phys. 16, 3289–3309. https://doi.org/10.5194/acp-16-3289-2016.

Arashiro, M., Lin, Y.H., Zhang, Z., Sexton, K.G., Gold, A., Jaspers, I., Fry, R.C., Surratt, J.D., 2018. Effect of secondary organic aerosol from isoprene-derived hydroxyhydroperoxides on the expression of oxidative stress response genes in human bronchial epithelial cells. Environ Sci Process Impacts 20, 332–339. https://doi.org/10.1039/c7em00439g.

Barcelona City Council, 2005. Anuari estadístic 2005.

Barcelona City Council, 2010. Anuari estadístic 2010.

Barcelona City Council, 2016. Anuari estadístic 2016.

Barcelona City Council, 2020. Construcción de viviendas [WWW Document]. http://www.bcn.cat/estadistica/castella/dades/timm/construccio/index.htm (accessed 2.9.21).

Bell, M.L., Ebisu, K., Leaderer, B.P., Gent, J.F., Lee, H.J., Koutrakis, P., Wang, Y., Dominici, F., Peng, R.D., 2014. Associations of PM2.5 constituents and sources with hospital admissions: analysis of four counties in Connecticut and Massachusetts (USA) for persons ≥ 65 years of age. Environ. Health Perspect. 122, 138–144. https://doi.org/10.1289/ehp.1306656.

Brines, M., Dall'Osto, M., Amato, F., Minguillón, M.C., Karanasiou, A., Grimalt, J.O., Alastuey, A., Querol, X., van Drooge, B.L., 2019. Source apportionment of urban PM1 in Barcelona during SAPUSS using organic and inorganic components. Environ. Sci. Pollut. Res. 26, 32114–32127. https://doi.org/10.1007/s11356-019-06199-3.

Carslaw, D.C., 2019. The Openair Manual Open-source Tools for Analysing Air Pollution Data. Manual for Version 2.6-6. University of York.

Carslaw, D.C., Ropkins, K., 2012. Openair - an r package for air quality data analysis. Environ. Model. Softw. 27–28, 52–61. https://doi.org/10.1016/j.envsoft.2011.09.008.

Cassee, F.R., Héroux, M.E., Gerlofs-Nijland, M.E., Kelly, F.J., 2013. Particulate matter beyond mass: recent health evidence on the role of fractions, chemical constituents and sources of emission. Inhal. Toxicol. 25, 802–812. https://doi.org/10.3109/08958378.2013.850127.

Castro, L.M., Pio, C.A., Harrison, R.M., Smith, D.J.T., 1999. Carbonaceous aerosol in urban and rural European atmospheres: estimation of secondary organic carbon concentrations. Atmos. Environ. 33, 2771–2781. https://doi.org/10.1016/S1352-2310(98)00331-8.

Cavalli, F., Putaud, J.P., 2010. Toward a standardized thermal-optical protocol for measuring atmospheric organic and elemental carbon: the eusaar protocol. ACS, Div. Environ. Chem. - Prepr. Ext. Abstr 48, 443–446. https://doi.org/10.5194/amtd-2-2321-2009.

Chow, J.C., Watson, J.G., Lowenthal, D.H., Magliano, K.L., 2005. Loss of PM2.5 nitrate from filter samples in central California. J. Air Waste Manage. Assoc. 55, 1158–1168. https://doi.org/10.1080/10473289.2005.10464704.

Chowdhury, P.H., He, Q., Carmieli, R., Li, C., Rudich, Y., Pardo, M., 2019. Connecting the oxidative potential of secondary organic aerosols with reactive oxygen species in exposed lung cells. Environ. Sci. Technol. 53, 13949–13958. https://doi.org/10.1021/acs.est.9b04449.

Cusack, M., Alastuey, A., Pérez, N., Pey, J., Querol, X., 2012. Trends of particulate matter (PM 2.5) and chemical composition at a regional background site in the Western Mediterranean over the last nine years (2002—2010). Atmos. Chem. Phys. 12, 8341–8357. https://doi.org/10.5194/acp-12-8341-2012.

Daellenbach, K.R., Uzu, G., Jiang, J., Cassagnes, L.-E., Leni, Z., Vlachou, A., Stefenelli, G., Canonaco, F., Weber, S., Segers, A., Kuenen, J.J.P., Schaap, M., Favez, O., Albinet, A., Aksoyoglu, S., Dommen, J., Baltensperger, U., Geiser, M., El Haddad, I., Jaffrezo, J.-L., Prévôt, A.S.H., 2020. Sources of particulate-matter air pollution and its oxidative potential in Europe. Nature 587, 414–419. https://doi.org/10.1038/s41586-020-2902-8.

Demographia World Urban Areas, 2020. Demographia World Urban Areas, 16th Annual Edition 2020.06. Demographia. p. 25.

Dias, D., Tchepel, O., Carvalho, A., Miranda, A.I., Borrego, C., 2012. Particulate matter and health risk under a changing climate: assessment for Portugal. Sci. World J. 2012, 10. https://doi.org/10.1100/2012/409546.

Dinoi, A., Cesari, D., Marinoni, A., Bonasoni, P., Riccio, A., Chianese, E., Tirimberio, G., Naccarato, A., Sprovieri, F., Andreoli, V., Moretti, S., Gullì, D., Calidonna, C.R., Ammoscato, I., Contini, D., 2017. Inter-comparison of carbon content in PM2.5 and PM10 collected at five measurement sites in Southern Italy. Atmosphere 8. https://doi.org/10.3390/atmos8120243.

DOE, 1992. Handbook of methods for the analysis of the various parameters of the carbon dioxide system in sea water. DOE Handb. 1994, p. 22.

EEA, 2018. Air Quality in Europe — 2018 Report. EEA Report No 12/2018. European Environmental Agency, Copenhagen https://doi.org/10.2800/777411.

EEA, 2020. Air quality in Europe - 2020 report. EEA Report.

Emami, F., Masiol, M., Hopke, P.K., 2018. Air pollution at Rochester, NY: long-term trends and multivariate analysis of upwind SO2 source impacts. Sci. Total Environ. 612, 1506–1515. https://doi.org/10.1016/j.scitotenv.2017.09.026.

EMEP/CCC, 2016. Air pollution trends in the EMEP region between 1990 and 2012. EMEP: CCC-Report 1/2016. Norwegian Institute for Air Research, Kjeller.

Escrig Vidal, A., Monfort, E., Celades, I., Querol, X., Amato, F., Minguillón, M.C., Hopke, P.K., 2009. Application of optimally scaled target factor analysis for assessing source contribution of ambient PM10. J. Air Waste Manage. Assoc. 59, 1296–1307. https://doi.org/10.3155/1047-3289.59.11.1296.

Escudero, M., Viana, M., Querol, X., Alastuey, A., Díez Hernández, P., García Dos Santos, S., Anzano, J., 2015. Industrial sources of primary and secondary organic aerosols in two urban environments in Spain. Environ. Sci. Pollut. Res. 22, 10413–10424. https://doi.org/10.1007/s11356-015-4228-x.

ETC/ACM, 2016. Long term air quality trends in Europe: contribution of meteorological variability. Natural Factors and Emissions 97.

European Commission, 2011. Establishing Guidelines for Demonstration and Subtraction of Exceedances Attributable to Natural Sources Under the Directive 2008/50/EC on Ambient Air Quality and Cleaner Air for Europe.

European Parliament, Council of the European Union, 2001. Directive 2001/80/EC of the European Parliament and of the Council of 23 October 2001 on the limitation of emissions of certain pollutants into the air from large combustion plants. Off. J. Eur. Union, 1–21 https://doi.org/10.1039/ap9842100196.

European Parliament, Council of the European Union, 2005. DIRECTIVE 2005/33/EC OF THE EUROPEAN PARLIAMENT AND OF THE COUNCIL of 6 July 2005 amending Directive 1999/32/EC. Off. J. Eur. Union 48 , 59–69.

European Parliament, Council of the European Union, 2008. Directive 2008/1/EC of the European Parliament and the Council of 15 January 2008 concerning integrated pollution prevention and control. Off. J. Eur. Union 24, 8–29.
Frey, H.C., 2018. Trends in onroad transportation energy and emissions. J. Air Waste Manage. Assoc. 68, 514–563. https://doi.org/10.1080/10962247.2018.1454357.
Grantz, D.A., Garner, J.H.B., Johnson, D.W., 2003. Ecological effects of particulate matter. Environ. Int. 29, 213–239. https://doi.org/10.1016/S0160-4120(02)00181-2.
Haynes, W.M., Lide, D.R., Bruno, T.J., 2017. Abundance of elements in the earth's crust and in the sea. CRC Handbook of Chemistry and Physics, pp. 14–17 Boca Raton, Florida.
Hime, N.J., Marks, G.B., Cowie, C.T., 2018. A comparison of the health effects of ambient particulate matter air pollution from five emission sources. Int. J. Environ. Res. Public Health 15, 1–24. https://doi.org/10.3390/ijerph15061206.
IHME, 2018. State of Global air 2018. https://doi.org/10.1143/JJAP.30.720.
IHME, 2020. Global burden of 87 risk factors in 204 countries and territories, 1990–2019: a systematic analysis for the Global Burden of Disease Study 2019. Lancet 396, 1223–1249. https://doi.org/10.1016/S0140-6736(20)30752-2.
Jalkanen, J.P., Johansson, L., Kukkonen, J., 2016. A comprehensive inventory of ship traffic exhaust emissions in the European sea areas in 2011. Atmos. Chem. Phys. 16, 71–84. https://doi.org/10.5194/acp-16-71-2016.
Jia, Y.Y., Wang, Q., Liu, T., 2017. Toxicity research of PM2.5 compositions in vitro. Int. J. Environ. Res. Public Health 14. https://doi.org/10.3390/ijerph14030232.
Jiang, H., Jang, M., Sabo-Attwood, T., Robinson, S.E., 2016. Oxidative potential of secondary organic aerosols produced from photooxidation of different hydrocarbons using outdoor chamber under ambient sunlight. Atmos. Environ. 131, 382–389. https://doi.org/10.1016/j.atmosenv.2016.02.016.
Kelly, F.J., Fussell, J.C., 2012. Size, source and chemical composition as determinants of toxicity attributable to ambient particulate matter. Atmos. Environ. 60, 504–526. https://doi.org/10.1016/j.atmosenv.2012.06.039.
Kirchstetter, T.W., Corrigan, C.E., Novakov, T., 2001. Laboratory and field investigation of the adsorption of gaseous organic compounds onto quartz filters. Atmos. Environ. 35, 1663–1671. https://doi.org/10.1016/S1352-2310(00)00448-9.
Marmer, E., Langmann, B., 2005. Impact of ship emissions on the Mediterranean summertime pollution and climate: a regional model study. Atmos. Environ. 39, 4659–4669. https://doi.org/10.1016/j.atmosenv.2005.04.014.
Massagué, J., Carnerero, C., Escudero, M., Baldasano, J.M., Alastuey, A., Querol, X., 2019. 2005-2017 ozone trends and potential benefits of local measures as deduced from air quality measurements in the north of the Barcelona Metropolitan Area. Atmos. Chem. Phys. Discuss., 1–28 https://doi.org/10.5194/acp-2019-33.
Minguillón, M.C., Perron, N., Querol, X., Szidat, S., Fahrni, S.M., Alastuey, A., Jimenez, J.L., Mohr, C., Ortega, A.M., Day, D.A., Lanz, V.A., Wacker, L., Reche, C., Cusack, M., Amato, F., Kiss, G., Hoffer, A., Decesari, S., Moretti, F., Hillamo, R., Teinilä, K., Seco, R., Peñuelas, J., Metzger, A., Schallhart, S., Müller, M., Hansel, A., Burkhart, J.F., Baltensperger, U., Prévôt, A.S.H., 2011. Fossil versus contemporary sources of fine elemental and organic carbonaceous particulate matter during the DAURE campaign in Northeast Spain. Atmos. Chem. Phys. 11, 12067–12084. https://doi.org/10.5194/acp-11-12067-2011.
Minguillón, M.C., Ripoll, A., Pérez, N., Prévôt, A.S.H., Canonaco, F., Querol, X., Alastuey, A., 2015. Chemical characterization of submicron regional background aerosols in the western Mediterranean using an Aerosol Chemical Speciation Monitor. Atmos. Chem. Phys. 15, 6379–6391. https://doi.org/10.5194/acp-15-6379-2015.
Ministerio para la Transición Ecológica, 2018. Evaluación de la calidad del aire en España.
Mohr, C., DeCarlo, P.F., Heringa, M.F., Chirico, R., Slowik, J.G., Richter, R., Reche, C., Alastuey, A., Querol, X., Seco, R., Peñuelas, J., Jiménez, J.L., Crippa, M., Zimmermann, R., Baltensperger, U., Prévôt, A.S.H., 2012. Identification and quantification of organic aerosol from cooking and other sources in Barcelona using aerosol mass spectrometer data. Atmos. Chem. Phys. 12, 1649–1665. https://doi.org/10.5194/acp-12-1649-2012.
Moreno, T., Querol, X., Alastuey, A., Reche, C., Cusack, M., Amato, F., Pandolfi, M., Pey, J., Richard, A., Prévt, A.S.H., Furger, M., Gibbons, W., 2011. Variations in time and space of trace metal aerosol concentrations in urban areas and their surroundings. Atmos. Chem. Phys. 11, 9415–9430. https://doi.org/10.5194/acp-11-9415-2011.
Norris, G., Duvall, R., Brown, S., Bai, S., 2014. EPA Positive Matrix Factorization (PMF) 5.0 Fundamentals and User Guide [WWW Document]. EPA.
Organization International Maritime, 2011. MARPOL Consolidated Edition 2011: Articles, Protocols, Annexes, Unified Interpretations of the International Convention for the Prevention of Pollution from Ships, 1973, as Modified by the 1978 and 1997 Protocols.
Paatero, P., Tapper, U., 1994. Positive matrix factorization: a non-negative factor model with optimal utilization of error estimates of data values. Environmetrics 5, 111–126.
Pachon, J.E., Weber, R.J., Zhang, X., Mulholland, J.A., Russell, A.G., 2013. Revising the use of potassium (K) in the source apportionment of PM2.5. Atmos. Pollut. Res. 4, 14–21. https://doi.org/10.5094/APR.2013.002.
Pandolfi, M., Amato, F., Reche, C., Alastuey, A., Otjes, R.P., Blom, M.J., Querol, X., 2012. Summer ammonia measurements in a densely populated Mediterranean city. Atmos. Chem. Phys. 12, 7557–7575. https://doi.org/10.5194/acp-12-7557-2012.
Pandolfi, M., Alastuey, A., Pérez, N., Reche, C., Castro, I., Shatalov, V., Querol, X., 2016. Trends analysis of PM source contributions and chemical tracers in NE Spain during 2004-2014: a multi-exponential approach. Atmos. Chem. Phys. 16, 11787–11805. https://doi.org/10.5194/acp-16-11787-2016.
Pandolfi, M., Mooibroek, D., Hopke, P., van Pinxteren, D., Querol, X., Herrmann, H., Alastuey, A., Favez, O., Hüglin, C., Perdrix, E., Riffault, V., Sauvage, S., van der Swaluw, E., Tarasova, O., Colette, A., 2020. Long range and local air pollution: what can we learn from chemical speciation of particulate matter at paired sites. Atmos. Chem. Phys. Discuss. 20, 409–429. https://doi.org/10.5194/acp-2019-493.
Park, M., Joo, H.S., Lee, K., Jang, M., Kim, S.D., Kim, I., Borlaza, L.J.S., Lim, H., Shin, H., Chung, K.H., Choi, Y.H., Park, S.G., Bae, M.S., Lee, J., Song, H., Park, K., 2018. Differential toxicities of fine particulate matters from various sources. Sci. Rep. 8, 1–11. https://doi.org/10.1038/s41598-018-35398-0.
Pérez, N., Pey, J., Castillo, S., Viana, M., Alastuey, A., Querol, X., 2008a. Interpretation of the variability of levels of regional background aerosols in the Western Mediterranean. Sci. Total Environ. 407, 527–540. https://doi.org/10.1016/j.scitotenv.2008.09.006.
Pérez, L., Tobias, A., Querol, X., Künzli, N., Pey, J., Viana, M., Valero, N., González-cabré, M., Sunyer, J., Perez, L., Tobias, A., Querol, X., Kunzli, N., Pey, J., Alastuey, A., Viana, M., Gonzdlez-cabre, N.V.M., Sunyer, J., 2008b. Coarse particles from Saharan dust and daily mortality winds from desert regions. Epidemiology 19, 800–807. https://doi.org/10.1097/EDE.0b013e3181813.
Pérez, N., Pey, J., Reche, C., Cortés, J., Alastuey, A., Querol, X., 2016. Impact of harbour emissions on ambient PM10 and PM2.5 in Barcelona (Spain): evidences of secondary aerosol formation within the urban area. Sci. Total Environ. 571, 237–250. https://doi.org/10.1016/j.scitotenv.2016.07.025.
Pey, J., Pérez, N., Querol, X., Alastuey, A., Cusack, M., Reche, C., 2010. Intense winter atmospheric pollution episodes affecting the Western Mediterranean. Sci. Total Environ. 408, 1951–1959. https://doi.org/10.1016/j.scitotenv.2010.01.052.
Pey, J., Querol, X., Alastuey, A., Forastiere, F., Stafoggia, M., 2013. African dust outbreaks over the Mediterranean Basin during 2001-2011: PM10 concentrations, phenomenology and trends, and its relation with synoptic and mesoscale meteorology. Atmos. Chem. Phys. 13, 1395–1410. https://doi.org/10.5194/acp-13-1395-2013.
Querol, X., Alastuey, A., Lopez-Soler, A., Plana, F., Mantilla, E., Juan, R., Ruiz, C.R., La Orden, A., 1999a. Characterisation of atmospheric particulates around a coal-fired power station. Int. J. Coal Geol. 40, 175–188. https://doi.org/10.1016/S0166-5162(98)00067-6.
Querol, X., Alastuey, A., Lopez-Soler, A., Plana, F., Puicercus, J.A., Mantilla, E., Palau, J.L., 1999b. Daily evolution of sulphate aerosols in a rural area, northeastern Spain-elucidation of an atmospheric reservoir effect. Environ. Pollut. 105, 397–407. https://doi.org/10.1016/S0269-7491(99)00037-8.
Querol, X., Alastuey, A., Rodriguez, S., Plana, F., Ruiz, C.R., Cots, N., Massagué, G., Puig, O., 2001a. PM10 and PM2.5 source apportionment in the Barcelona Metropolitan area, Catalonia, Spain. Atmos. Environ. 35, 6407–6419. https://doi.org/10.1016/S1352-2310(01)00361-2.
Querol, X., Alastuey, H., Rodriguez, S., Mantilla, E., Ruiz, C.R., 2001b. Monitoring of PM10 and PM2.5 around primary particulate anthropogenic emission sources. Atmos. Environ. 35, 845–858.
Querol, X., Alastuey, A., Ruiz, C.R., Artiñano, B., Hansson, H.C., Harrison, R.M., Buringh, E., Ten Brink, H.M., Lutz, M., Bruckmann, P., Straehl, P., Schneider, J., 2004a. Speciation and origin of PM10 and PM2.5 in selected European cities. Atmos. Environ. 38, 6547–6555. https://doi.org/10.1016/j.atmosenv.2004.08.037.
Querol, X., Alastuey, A., Viana, M.M., Rodriguez, S., Artiñano, B., Salvador, P., Garcia Do Santos, S., Fernandez Patier, R., Ruiz, C.R., De La Rosa, J., Sanchez De La Campa, A., Menendez, M., Gil, J.I., 2004b. Speciation and origin of PM10 and PM2.5 in Spain. J. Aerosol Sci. 35, 1151–1172. https://doi.org/10.1016/j.jaerosci.2004.04.002.
Querol, X., Viana, M., Alastuey, A., Amato, F., Moreno, T., Castillo, S., Pey, J., de la Rosa, J., Sánchez de la Campa, A., Artíñano, B., Salvador, P., García Dos Santos, S., Fernández-Patier, R., Moreno-Grau, S., Negral, L., Minguillón, M.C., Monfort, E., Gil, J.I., Inza, A., Ortega, L.A., Santamaría, J.M., Zabalza, J., 2007. Source origin of trace elements in PM from regional background, urban and industrial sites of Spain. Atmos. Environ. 41, 7219–7231. https://doi.org/10.1016/j.atmosenv.2007.05.022.
Querol, X., Alastuey, A., Moreno, T., Viana, M.M., Castillo, S., Pey, J., Rodríguez, S., Artiñano, B., Salvador, P., Sánchez, M., Garcia Dos Santos, S., Herce Garraleta, M.D., Fernandez-Patier, R., Moreno-Grau, S., Negral, L., Minguillón, M.C., Monfort, E., Sanz, M.J., Palomo-Marín, R., Pinilla-Gil, E., Cuevas, E., de la Rosa, J., Sánchez de la Campa, A., 2008. Spatial and temporal variations in airborne particulate matter (PM10 and PM2.5) across Spain 1999-2005. Atmos. Environ. 42, 3964–3979. https://doi.org/10.1016/j.atmosenv.2006.10.071.
Querol, X., Alastuey, A., Pey, J., Cusack, M., Pérez, N., Mihalopoulos, N., Theodosi, C., Gerasopoulos, E., Kubilay, N., Koçak, M., 2009a. Variability in regional background aerosols within the Mediterranean. Atmos. Chem. Phys. 9, 4575–4591. https://doi.org/10.5194/acp-9-4575-2009.
Querol, X., Pey, J., Pandolfi, M., Alastuey, A., Cusack, M., Pérez, N., Moreno, T., Viana, M., Mihalopoulos, N., Kallos, G., Kleanthous, S., 2009b. African dust contributions to mean ambient PM10 mass-levels across the Mediterranean Basin. Atmos. Environ. 43, 4266–4277. https://doi.org/10.1016/j.atmosenv.2009.06.013.
Querol, X., Alastuey, A., Viana, M., Moreno, T., Reche, C., Minguillón, M.C., Ripoll, A., Pandolfi, M., Amato, F., Karanasiou, A., Pérez, N., Pey, J., Cusack, M., Vázquez, R., Plana, F., Dall'Osto, M., De La Rosa, J., Sánchez De La Campa, A., Fernández-Camacho, R., Rodríguez, S., Pio, C., Alados-Arboledas, L., Titos, G., Artíñano, B., Salvador, P., García Dos Santos, S., Fernández Patier, R., 2013. Variability of carbonaceous aerosols in remote, rural, urban and industrial environments in Spain: implications for air quality policy. Atmos. Chem. Phys. 13, 6185–6206. https://doi.org/10.5194/acp-13-6185-2013.
Querol, X., Alastuey, A., Pandolfi, M., Reche, C., Pérez, N., Minguillón, M.C., Moreno, T., Viana, M., Escudero, M., Orio, A., Pallarés, M., Reina, F., 2014. 2001-2012 trends on air quality in Spain. Sci. Total Environ. 490, 957–969. https://doi.org/10.1016/j.scitotenv.2014.05.074.
Querol, X., Alastuey, A., Reche, C., Orio, A., Pallares, M., Reina, F., Dieguez, J.J., Mantilla, E., Escudero, M., Alonso, L., Gangoiti, G., Millán, M., 2016. On the origin of the highest ozone episodes in Spain. Sci. Total Environ. 572, 379–389. https://doi.org/10.1016/j.scitotenv.2016.07.193.
Querol, X., Pérez, N., Reche, C., Ealo, M., Ripoll, A., Tur, J., Pandolfi, M., Pey, J., Salvador, P., Moreno, T., Alastuey, A., 2019. African dust and air quality over Spain: is it only dust that matters? Sci. Total Environ. 686, 737–752. https://doi.org/10.1016/j.scitotenv.2019.05.349.
Reche, C., Viana, M., Amato, F., Alastuey, A., Moreno, T., Hillamo, R., Teinilä, K., Saarnio, K., Seco, R., Peñuelas, J., Mohr, C., Prévôt, A.S.H., Querol, X., 2012. Biomass burning

contributions to urban aerosols in a coastal Mediterranean City. Sci. Total Environ. 427–428, 175–190. https://doi.org/10.1016/j.scitotenv.2012.04.012.
Reche, C., Viana, M., Karanasiou, A., Cusack, M., Alastuey, A., Artiñano, B., Revuelta, M.A., López-Mahía, P., Blanco-Heras, G., Rodríguez, S., Sánchez de la Campa, A.M., Fernández-Camacho, R., González-Castanedo, Y., Mantilla, E., Tang, Y.S., Querol, X., 2015. Urban NH3 levels and sources in six major Spanish cities. Chemosphere 119, 769–777. https://doi.org/10.1016/j.chemosphere.2014.07.097.
Rodríguez, S., Querol, X., Alastuey, A., Mantilla, E., 2002. Origin of high summer PM10 and TSP concentrations at rural sites in Eastern Spain. Atmos. Environ. 36, 3101–3112. https://doi.org/10.1016/S1352-2310(02)00256-X.
Saiz-Lopez, A., Borge, R., Notario, A., Adame, J.A., La Paz, D.D., Querol, X., Artíñano, B., Gómez-Moreno, F.J., Cuevas, C.A., 2017. Unexpected increase in the oxidation capacity of the urban atmosphere of Madrid, Spain. Sci. Rep. 7, 1–11. https://doi.org/10.1038/srep45956.
Seco, R., Peñuelas, J., Filella, I., Llusià, J., Molowny-Horas, R., Schallhart, S., Metzger, A., Müller, M., Hansel, A., 2011. Contrasting winter and summer VOC mixing ratios at a forest site in the Western Mediterranean Basin: the effect of local biogenic emissions. Atmos. Chem. Phys. 11, 13161–13179. https://doi.org/10.5194/acp-11-13161-2011.
Sen, P.K., 1968. Estimates of the regression coefficient based on Kendall's Tau. J. Am. Stat. Assoc. 63, 1379–1389. https://doi.org/10.1080/01621459.1968.10480934.
Squizzato, S., Masiol, M., Rich, D.Q., Hopke, P.K., 2018. A long-term source apportionment of PM2.5 in New York State during 2005–2016. Atmos. Environ. 192, 35–47. https://doi.org/10.1016/j.atmosenv.2018.08.044.
Sutton, M.A., Reis, S., Riddick, S.N., Dragosits, U., Nemitz, E., Theobald, M.R., Tang, Y.S., Braban, C.F., Vieno, M., Dore, A.J., Mitchell, R.F., Wanless, S., Daunt, F., Fowler, D., Blackall, T.D., Milford, C., Flechard, C.R., Loubet, B., Massad, R., Cellier, P., Personne, E., Coheur, P.F., Clarisse, L., Van Damme, M., Ngadi, Y., Clerbaux, C., Skjøth, C.A., Geels, C., Hertel, O., Kruit, R.J.W., Pinder, R.W., Bash, J.O., Walker, J.T., Simpson, D., Horváth, L., Misselbrook, T.H., Bleeker, A., Dentener, F., de Vries, W., 2013. Towards a climate-dependent paradigm of ammonia emission and deposition. Philos. Trans. R. Soc. B Biol. Sci. 368. https://doi.org/10.1098/rstb.2013.0166.
Theil, H., 1950. A rank-invariant method of linear and polynomial regression analysis, i, ii, iii. Proceedings of the Koninklijke Nederlandse Akademie Wetenschappen.
Tsyro, S.G., 2005. To what extent can aerosol water explain the discrepancy between model calculated and gravimetric PM_{10} and $PM_{2.5}$? Atmos. Chem. Phys. 5, 515–532. https://doi.org/10.5194/acp-5-515-2005.
Tuet, W.Y., Chen, Y., Xu, L., Fok, S., Gao, D., Weber, R.J., Ng, N.L., 2017. Chemical oxidative potential of secondary organic aerosol (SOA) generated from the photooxidation of biogenic and anthropogenic volatile organic compounds. Atmos. Chem. Phys. 17, 839–853. https://doi.org/10.5194/acp-17-839-2017.
Turpin, B.J., Lim, H.J., 2001. Species contributions to pm2.5 mass concentrations: revisiting common assumptions for estimating organic mass. Aerosol Sci. Technol. 35, 602–610. https://doi.org/10.1080/02786820119445.
Turpin, B.J., Saxena, P., Allen, G., Koutrakis, P., McMurry, P., Hildemann, L., 1997. Characterization of the southwestern desert aerosol, meadview, az. J. Air Waste Manage. Assoc. 47, 344–356. https://doi.org/10.1080/10473289.1997.10464451.
UNECE, 2016. Towards Cleaner Air. Scientific Assessment Report 2016 (Oslo).
Van Damme, M., Clarisse, L., Whitburn, S., Hadji-Lazaro, J., Hurtmans, D., Clerbaux, C., Coheur, P.F., 2018. Industrial and agricultural ammonia point sources exposed. Nature 564, 99–103. https://doi.org/10.1038/s41586-018-0747-1.
Via, M., Minguillón, M.C., Reche, C., Querol, X., Alastuey, A., 2021. Increase of secondary organic aerosol over four years in an urban environment. Atmos. Chem. Phys. Discuss. 1–20.
Viana, M., Chi, X., Maenhaut, W., Querol, X., Alastuey, A., Mikuška, P., Večeřa, Z., 2006. Organic and elemental carbon concentrations in carbonaceous aerosols during summer and winter sampling campaigns in Barcelona, Spain. Atmos. Environ. 40, 2180–2193. https://doi.org/10.1016/j.atmosenv.2005.12.001.
Viana, M., Reche, C., Amato, F., Alastuey, A., Querol, X., Moreno, T., Lucarelli, F., Nava, S., Calzolai, G., Chiari, M., Rico, M., 2013. Evidence of biomass burning aerosols in the Barcelona urban environment during winter time. Atmos. Environ. 72, 81–88. https://doi.org/10.1016/j.atmosenv.2013.02.031.
Viana, M., Hammingh, P., Colette, A., Querol, X., Degraeuwe, B., Vlieger, I. de, van Aardenne, J., 2014. Impact of maritime transport emissions on coastal air quality in Europe. Atmos. Environ. 90, 96–105. https://doi.org/10.1016/j.atmosenv.2014.03.046.
Wang, S., Ye, J., Soong, R., Wu, B., Yu, L., Simpson, A.J., Chan, A.W.H., 2018. Relationship between chemical composition and oxidative potential of secondary organic aerosol from polycyclic aromatic hydrocarbons. Atmos. Chem. Phys. 18, 3987–4003. https://doi.org/10.5194/acp-18-3987-2018.
Wang, H., Tang, R., Shen, R., Yu, Y., Liu, K., Tan, R., Zhang, W., 2020. Secondary Organic Aerosol Formation from On-road Gasoline Vehicles in China 8093.
Watson, J.G., Chow, J.C., Chen, L.W.A., Frank, N.H., 2009. Methods to assess carbonaceous aerosol sampling artifacts for IMPROVE and other long-term networks. J. Air Waste Manage. Assoc. 59, 898–911. https://doi.org/10.3155/1047-3289.59.8.898.
WHO, 2006. WHO air quality guidelines for particulate matter, ozone, nitrogen dioxide and sulfur dioxide: global update 2005: summary of risk assessment. World Health Organization.
WHO, 2013. Review of Evidence on Health Aspects of Air Pollution - REVIHAAP Project. https://doi.org/10.1007/BF00379640.
WHO, 2016. Ambient air pollution: a global assessment of exposure and burden of disease. World Health Organization.
WHO, 2018. Burden of Disease from Ambient Air Pollution for 2016.
Wu, C., Yu, J.Z., 2016. Determination of primary combustion source organic carbon-to-elemental carbon (OC / EC) ratio using ambient OC and EC measurements: secondary OC-EC correlation minimization method. Atmos. Chem. Phys. 16, 5453–5465. https://doi.org/10.5194/acp-16-5453-2016.
Yu, S., Dennis, R.L., Bhave, P.V., Eder, B.K., 2004. Primary and secondary organic aerosols over the United States: estimates on the basis of observed organic carbon (OC) and elemental carbon (EC), and air quality modeled primary OC/EC ratios. Atmos. Environ. 38, 5257–5268. https://doi.org/10.1016/j.atmosenv.2004.02.064.
Yu, J., Yan, C., Liu, Y., Li, X., Zhou, T., Zheng, M., 2018. Potassium: a tracer for biomass burning in Beijing? Aerosol Air Qual. Res. 18, 2447–2459. https://doi.org/10.4209/aaqr.2017.11.0536.
Zhang, H., Li, Z., Liu, Y., Xinag, P., Cui, X.Y., Ye, H., Hu, B.L., Lou, L.P., 2018a. Physical and chemical characteristics of PM2.5 and its toxicity to human bronchial cells BEAS-2B in the winter and summer. J Zhejiang Univ Sci B 19, 317–326. https://doi.org/10.1631/jzus.B1700123.
Zhang, W., Lin, S., Hopke, P.K., Thurston, S.W., van Wijngaarden, E., Croft, D., Squizzato, S., Masiol, M., Rich, D.Q., 2018b. Triggering of cardiovascular hospital admissions by fine particle concentrations in New York state: before, during, and after implementation of multiple environmental policies and a recession. Environ. Pollut. 242, 1404–1416. https://doi.org/10.1016/j.envpol.2018.08.030.
Zhao, Y., Saleh, R., Saliba, G., Presto, A.A., Gordon, T.D., Drozd, G.T., Goldstein, A.H., Donahue, N.M., Robinson, A.L., 2017. Reducing secondary organic aerosol formation from gasoline vehicle exhaust. Proc. Natl. Acad. Sci. U. S. A. 114, 6984–6989. https://doi.org/10.1073/pnas.1620911114.